06

E/S No. C-1031

III

A STUDY OF MESOSCALE SURFACE HEAT AND MOISTURE BUDGETS AND THEIR RELATIONSHIP TO AIRMASS CUMULUS CLOUDS OBSERVED IN LANDSAT IMAGERY

R. R. Sabatini
E. S. Merritt
W. D. Hart
L. J. Heitkemper
D. L. Hlavka

Earth Satellite Corporation (EarthSat)
7222 47th St. (Chevy Chase)
Washington, D. C. 20015

October 1976

Final Report for Period February 1975 - October 1976

21540

Prepared for

GODDARD SPACE FLIGHT CENTER
Greenbelt, Maryland 20771

TECHNICAL REPORT STANDARD TITLE PAGE

1. Report No.	2. Government Accession No.	3. Recipient's Catalog No.

4. Title and Subtitle
A Study of Mesoscale Surface Heat and Moisture Budgets and Their Relationship to Airmass Cumulus Clouds Observed in Landsat Imagery

5. Report Date
October 1976

6. Performing Organization Code

7. Author(s) R.R. Sabatini, E.S. Merritt, L. Heitkemper, W.D. Hart, D.L. Hlavka

8. Performing Organization Report No.
C-1031

9. Performing Organization Name and Address
Earth Satellite Corporation
7222 47th Street (Chevy Chase)
Washington, D.C. 20015

10. Work Unit No.

11. Contract or Grant No.
NAS5-20944

13. Type of Report and Period Covered
Final Report
Feb. '75 - Oct. '76

12. Sponsoring Agency Name and Address
NASA Goddard Space Flight Center
Greenbelt, Maryland 20771
Technical Monitor - Harold Oseroff

14. Sponsoring Agency Code

15. Supplementary Notes
Original photography may be purchased from
EROS Data Center
10th and Dakota Avenue
Sioux Falls, SD 57198

16. Abstract

The primary objective of this study has been to determine the influence of the surface heat and moisture budgets on the formation of cumulus clouds within a uniform air mass in an area of the central U.S. The achievement of this primary objective has necessitated the adaptation and further development of schemes for computing surface budgets from standard meteorological observations. Thus, a secondary objective has been the modification of these schemes to fit the available data. Another secondary objective has been the development of a scheme to use the Landsat data for estimating the surface albedo. Standard climatological data and information on land use enabled us to perform budget calculations for three Landsat scenes in the Central U.S. The contribution of Landsat to this study has been to furnish (1) fine resolution cloud cover, (2) background albedo for the net radiation calculations, (3) information on vegetation cover. The three budget analyses performed show a weak correspondence between Landsat cloud patterns and elements of the energy and moisture budgets. We do find that a little more energy is contributed by the ground to heat the air in cloudy areas. Improvements are warranted in the budget models and data coverage necessary to describe the environment. Our models can serve as basis for more complex models of surface-air heat and moisture exchanges which would utilize readily available meteorological data on a mesoscale.

17. Key Words (Selected by Author(s))	18. Distribution Statement
SURFACE HEAT AND MOISTURE BUDGETS LANDSAT	Unlimited

19. Security Classif. (of this report)	20. Security Classif. (of this page)	21. No. of Pages	22. Price*
Unclassified		86	

*For sale by the Clearinghouse for Federal Scientific and Technical Information, Springfield, Virginia 22151.

PREFACE

The primary objective of this study has been to determine the influence of the surface heat and moisture budgets on the formation of cumulus clouds within a uniform air mass in an area of the central U.S. The achievement of this primary objective has necessitated the adaptation and further development of schemes for computing surface budgets from standard meteorological observations including the development of an algorithm to use the Landsat data for estimating the surface albedo.

Standard climatological data and information on land use enabled us to perform budget calculations for three Landsat scenes in the central U.S.

The contribution of Landsat to this study has been to furnish (1) fine resolution cloud cover, (2) background albedo for the net radiation calculations, and (3) information on vegetation cover.

The budget analyses show a weak correspondence between Landsat cloud patterns and elements of the energy and moisture budgets. We find that more energy is contributed by the ground to heat the air in cloudy areas.

Improvements are required in the budget models and data coverage. The models can serve as a basis for development of more complex models of surface-air heat and moisture exchanges which would utilize readily available meteorological data on a mesoscale.

Specific recommendations are (1) improvements in the surface heat and soil moisture budget models, and (2) improvements in the data base and model calibration.

Improvements in the budget models can be achieved by inclusion of (1) a ground heat storage term, (2) horizontal heat transport, and (3) turbulent mixing due to horizontal mass convection and surface roughness. Improvements in our data base can be achieved by the use of meteorological satellite data and the inclusion of ground observations of evaporation (from lysimeter sites) and solar radiation for a check on the model's estimates of solar radiation and evaporation.

The resources under this contract did not permit us to fully explore the applicability of meteorological satellite data to the calculation of the surface heat and moisture budgets. Satellite cloud cover (such as discernible from SMS images) can be useful, for example, to estimate solar radiation and to improve precipitation estimates. Satellite infrared measurements, properly corrected for the atmosphere and surface emissivity, can yield surface temperatures in clear areas, which can then be used to improve surface net radiation and evaporation estimates. The integration of meteorological satellite data and surface observations in an improved version of the heat and moisture budget model would permit daily and hour-to-hour monitoring of air mass exchange processes over large areas.

TABLE OF CONTENTS

LIST OF ILLUSTRATIONS

LIST OF ILLUSTRATIONS (CONT'D)

LIST OF ILLUSTRATIONS (CONCLUDED)

LIST OF TABLES

1.0 INTRODUCTION

Small scale cumuliform cloudiness associated with both tropical and polar air masses which have penetrated into various regions of the midwestern U.S. have been observed in Landsat imagery. These images reveal substantial spatial variability in the cumuliform cloud density and size over reasonably uniform land forms.

The primary objective of this study has been to determine the influence of the surface heat and moisture budgets on the formation of cumulus cloud cover within a uniform air mass newly established in an area of the central U.S. The achievement of this primary objective has necessitated the adaptation and further development of schemes for computing surface heat and moisture budgets from standard meteorological observations. These schemes, which have been developed by Earth Satellite Corporation for its crop yield forecasting system, CROPCAST^{TM}, have already been described in detail in various publications (Earth Satellite Corporation, 1975, 1976). Thus, a secondary objective has been the modification of these existing systems for calculating surface heat and moisture budgets from standard meteorological observations. Another secondary objective has been the development of a scheme to use the Landsat data itself for estimating the total surface albedo, which is an input to the budget calculations. It was at first proposed to concentrate this study in areas in which lysimeter sites are located, with the intention to use the evaporation reported at the lysimeter site as a check on calculations of evaporation done with standard climatological data. However, the unavailability of lysimeter data limited us to the use of climatological data for the estimation of evaporation. Within the three 185 x 185 km Landsat scenes in the central U.S. used for our

study, we have available 19 to 21 cooperative climatological stations reporting daily maximum and minimum temperatures and precipitation, and one first order weather station additionally reporting dew point temperatures, wind, and cloud cover. These data, coupled with some information on land use enabled us to perform large area heat and moisture budget calculations which, by any previous standard, are spatially very detailed. Since the amount of evaporation establishes how much energy is left to heat the air for convection, an accurate determination of evaporation is necessary. To achieve the needed accuracy one needs spatially detailed information on (1) the available energy to evaporate the water; (2) the amount of water in the soil; and (3) type and conditions of plant surfaces. Thus, the success of our study depends on a physically sound computational model which correctly describes the processes that determine how much energy is left to heat the air, and on the availability of the data necessary to describe the environment. The approach we have taken combines relative simplicity of computational model to the availability of meteorological data on a synoptic scale.

The contribution of Landsat data to this study has been to furnish (1) fine resolution cloud cover data on a mesoscale; and (2) background albedo for the net radiation calculations. Landsat data can also offer additional information on vegetation cover which is probably the most important factor controlling evaporation, and on surface roughness which is a factor determining small cumulus formation.

The three heat and moisture budget analyses we have performed show a weak correspondence between cloud patterns and elements of the energy and moisture budgets. We do find that there is a little more energy contributed by the ground to heat the air in cloudy areas. These

results are encouraging, nevertheless improvements are warranted both in the heat and moisture budget model and in the data coverage necessary to describe the environment.

Section 2 describes the data employed in our study. Section 3 describes our heat and moisture budget model, and the results of the calculations. Sections 4 and 5 conclude with a summary and recommendations which include improvements on the model and on the data base.

2.0 DESCRIPTION OF DATA AND DATA SEARCH

2.1 Search for Landsat Images Containing Cumuliform Clouds

Our first search for Landsat images conducted in May 1975 at GSFC, concentrated for images around locations in the U.S. that were furnished with lysimeters. The search was limited to those cumuliform cloud patterns that seemed to have been caused by local effects and air mass modification. Cloud cover was in all cases to be less than 50%. Another limitation we imposed on the search was the presence of a clear or mostly clear background image of the same area occuring within $\pm$ 54 days. This background image was needed to better define surface albedo in cloudy areas.

This first search yielded 12 possible cases, five of which we eliminated because of the nearness of fronts or instability lines that may have masked local effects on cloud formation. We then ordered Computer Compatible Tapes from the Landsat Data Center, Sioux Falls, S.D., for the remaining cases and their respective background images. We also ordered 1:1,000,000 black-and-white images from the Environmental Data Service, Suitland, Md. After receiving these data, we learned that the lysimeter measurements would not be available in time for our use. To compensate for this loss of data necessary for accurate heat and moisture budget calculations, we searched the NOAA Monthly Climatological Summaries for daily meteorological data in the areas of interest. During this search we found several areas in the U.S. other than the lysimeter sites, with sufficient climatological data. We therefore opted to make another search for Landsat data over these areas. This second search conducted in February 1976, enabled us to include Landsat 2 data in the study.

Table 2-1 lists the final three cases selected for a complete heat and moisture budget analysis, and their background images.

Figures 2-1 to 2-5 shows the 1:1,000,000 Landsat images of the areas selected and their background images. No background image was deemed necessary for the 5 July 1975 case, because of little cloud cover. We also ordered 1:250,000 black-and-white Band 5 prints of these images to permit a better evaluation of the cloud patterns.

Since the 5 July 1975 case was selected rather late in the study, the computer tape was not obtained in time to process an albedo map. However, estimates of surface albedoes from like areas in the other two cases permitted us to complete a budget study for this third case.

2.2 Landsat Data Tapes and Processing

The digital Landsat data used in this project are on 9-track, 1600 BPI Computer Compatible Tapes (CCT). Each tape has four files containing data from one Landsat image. Each file holds data for one 46.4 km x 185 km strip from the Landsat image and contains 2,340 data records or lines with 3,240 bytes of Landsat data plus up to 56 bytes of annotation information. Since there are four bytes of information for each pixel*, there are a total of (2,340 x 3,240)/4 = 1,895,400 pixels in each strip. The entire tape thus has 30,326,400 bytes of information from 7,581,600 pixels.

*A pixel is a single resolution element in a channel of the MSS.

Table 2-1

Selected Landsat Data for Study

Landsat	Scene ID	Area	Date	Time (GMT)
I	1652-16334	Manhattan, Kansas	6 May 1974*	16:33
I	1670-16331	Manhattan, Kansas	24 May 1974	16:33
II	2144-16282	Manhattan, Kansas	15 June 1975*	16:28
II	2162-16282	Manhattan, Kansas	3 July 1975	16:28
II	2164-16372	Fargo, N.D.	5 July 1975	16:37

*Images and data used for background albedo in cloudy areas.

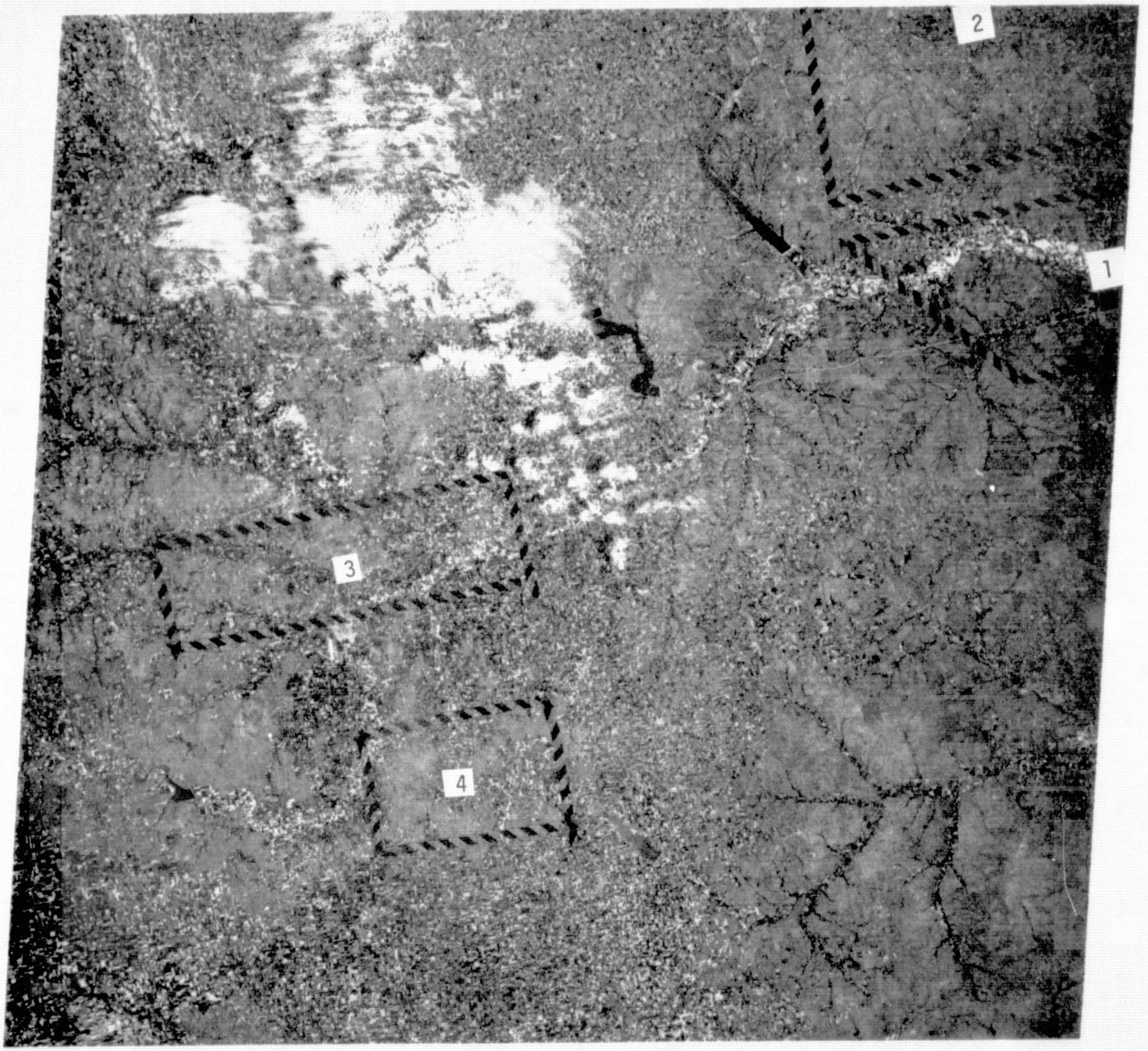

Figure 2-1: MSS-5 image of the Manhattan, Kansas area taken by the Landsat-1 satellite on 6 May 1974. Average albedoes were calculated for the rectangular areas shown, as discussed in Section 3.3.

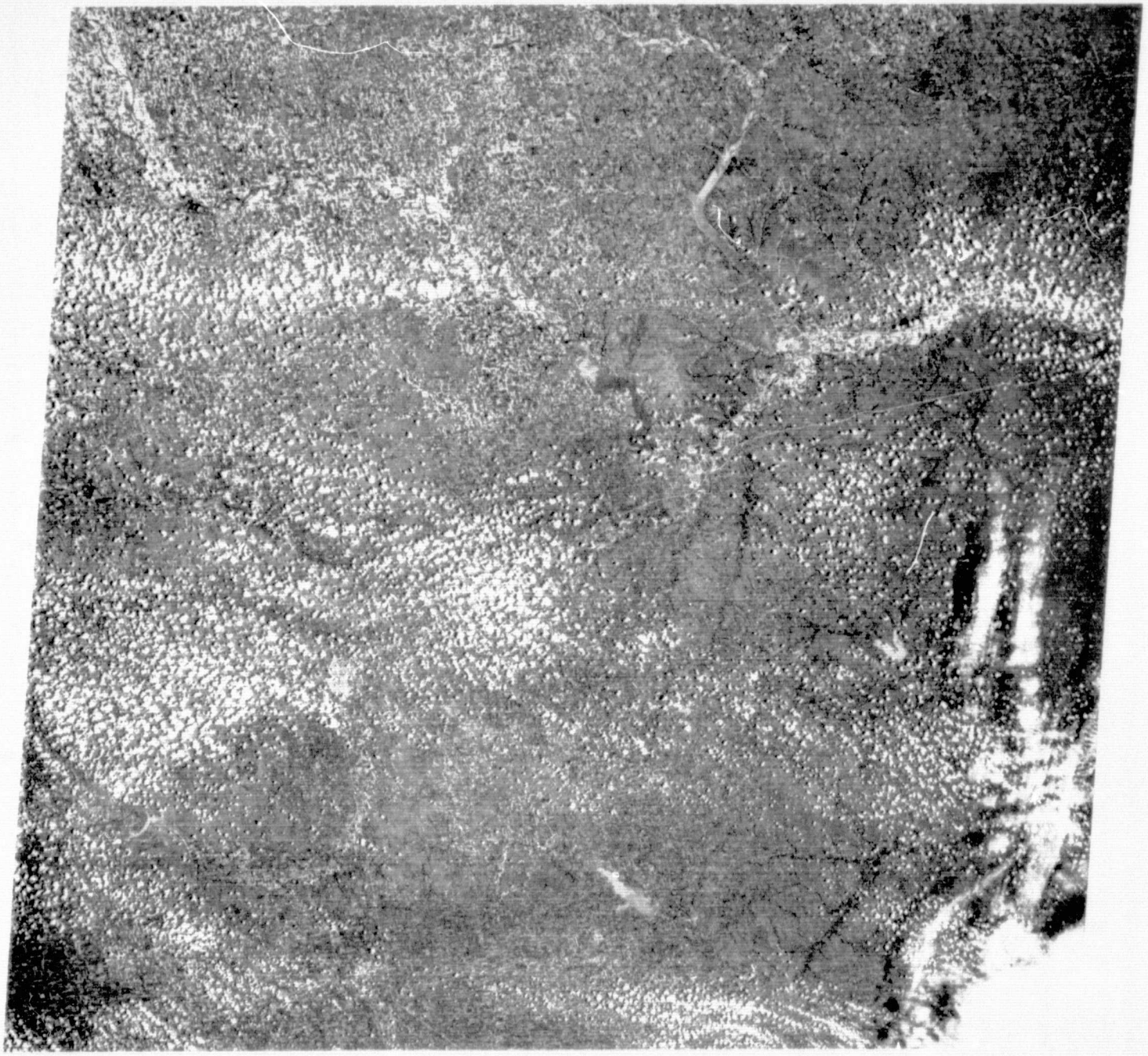

Figure 2-2: MSS-5 image of the Manhattan, Kansas area taken by the Landsat-1 satellite on 24 May 1974.

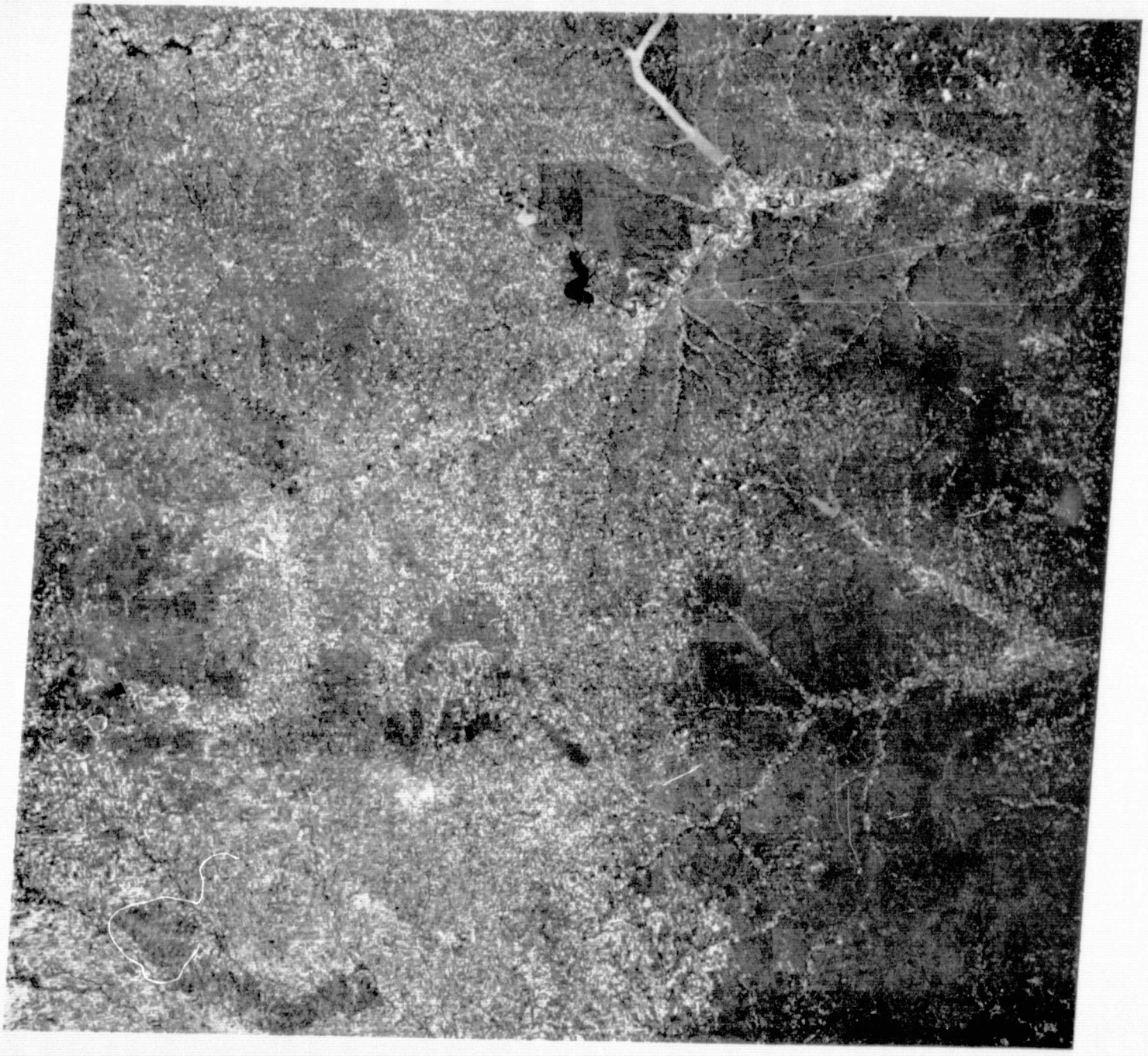

Figure 2-3: MSS-5 image of the Manhattan, Kansas area taken by the Landsat-2 satellite on 15 June 1975.

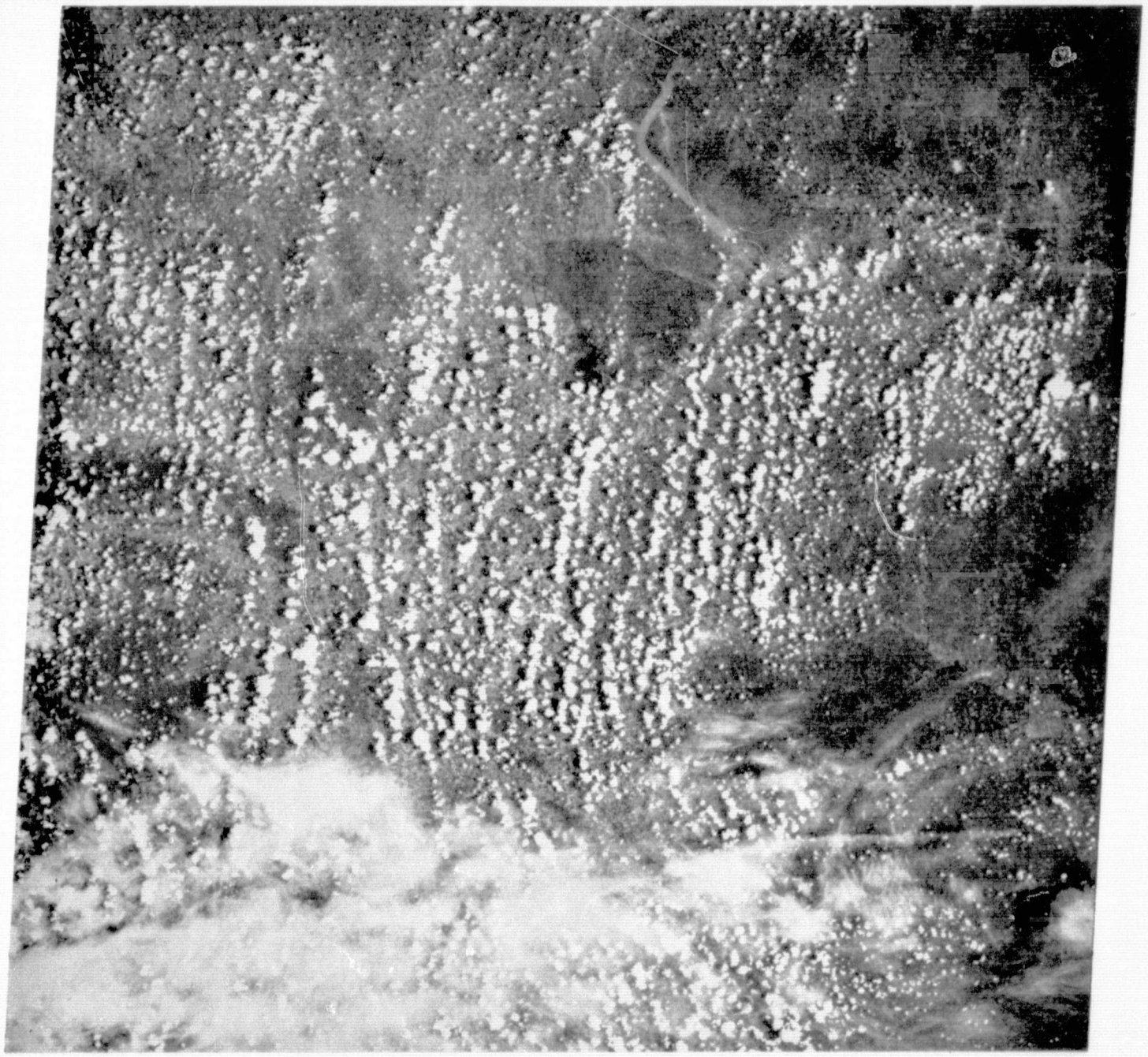

Figure 2-4: MSS-5 image of the Manhattan, Kansas area taken by the Landsat-2 satellite on 3 July 1975.

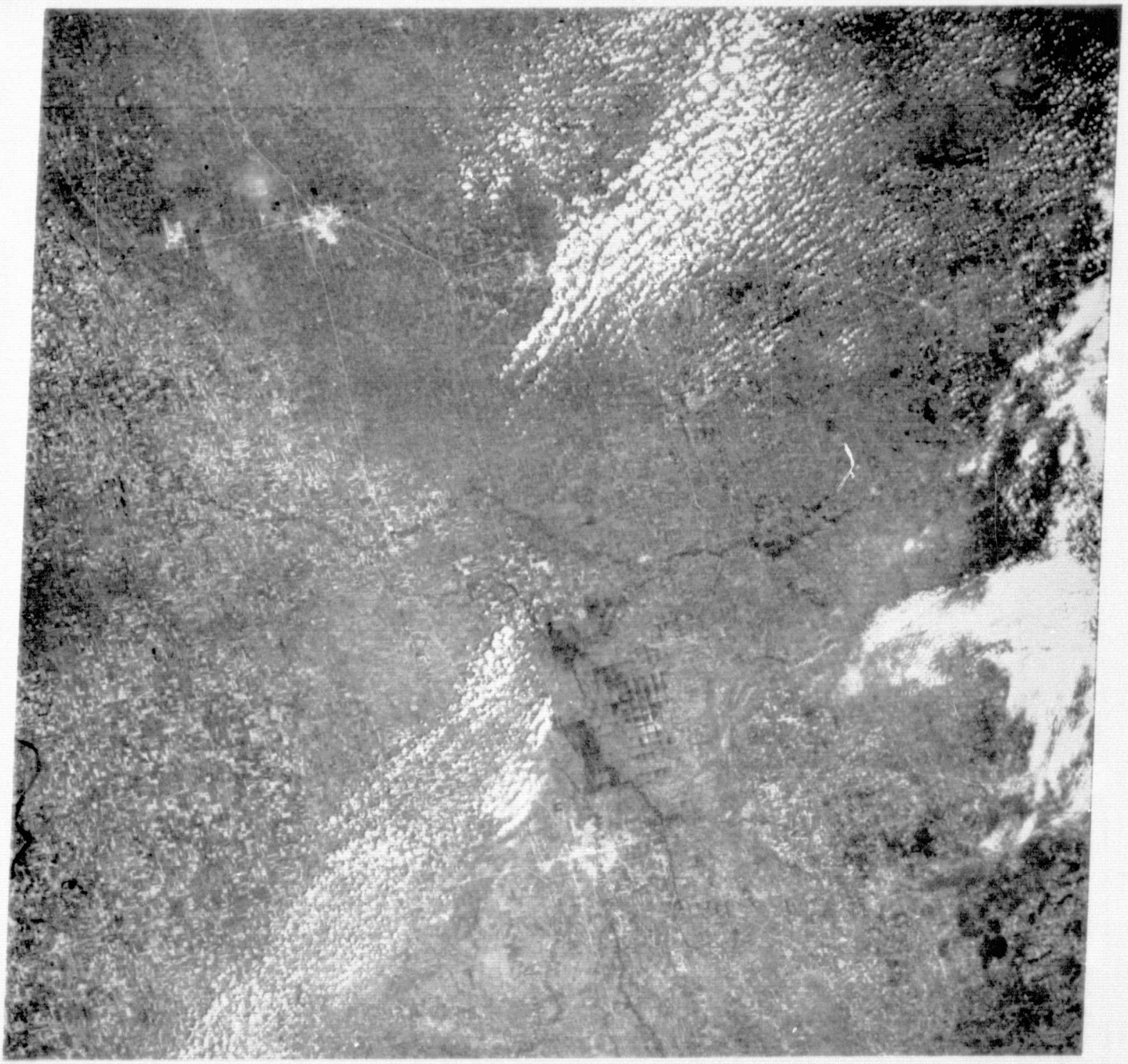

Figure 2-5: MSS-5 image of the Fargo, N.D. area taken by the Landsat-2 satellite on 5 July 1975.

The data for each pixel are calibrated counts C_i from each MSS channels 4, 5, 6, or 7 (Bands 1, 2, 3, 4) which are translatable to radiances, R_i, by

$$R_i = R_{max,i}\ C_i/C_{max,i}$$

where $R_{max,i}$ and $C_{max,i}$ are the maximum radiances and counts for each MSS Band, i, shown in Table 2-2.

The Landsat tapes are read by an assembler language subroutine called READER which translates the 3,296 bytes of each data line into 3,296 half words. The use of subroutine READER has two advantages: 1) the input-output efficiency is increased by a factor of about ten over the use of a conventional FORTRAN subroutine, and 2) the data are translated into a form directly usable by a FORTRAN program.

A FORTRAN language computer program then processes the Landsat data fetched by subroutine READER. This program calculated albedoes by using radiances measured by the MSS bands as described in Section 3.

The calculated albedoes represent average values for areas approximately 3.4 km^2 (1 sq. n.m.). These averages are obtained by sampling 16 out of the total 736 (32 x 23) radiance values contained in 3.4 km^2 area. To accomplish this sampling, the program is written to access every eighth datum in every sixth line of Landsat data. This spacing of data selection represents about 3.4 km^2 on the earth resulting in 16 values for each 3.4 km^2.

Table 2-2

MSS Maximum Radiance and Counts

Band	Rmax $mwcm^{-2}sr^{-1}$	Cmax counts
1	2.48	127
2	2.00	127
3	1.76	127
4	4.60	63

Reference: NASA Earth Resources Satellite, Data Users Handbook, Appendix A (1972)

This sampling technique saves much computing time while still maintaining adequate resolution and accuracy. By use of Chebycheff's inequality (Freund, 1970) we estimated that a mean from a sample of 16 values has a probability of at least 0.93 of being within one standard deviation of the true mean and a probability of at least 0.75 of being within onehalf standard deviation of the true mean (the true mean being the 736 values mean).

2.3 Surface Climatological Data

The location of climatological stations used for the heat and soil moisture budgets in the three selected cases are shown in Figures 2-6, 2-7, 2-8. The required meteorological data for our computer routines which perform the heat budget calculations are six-hourly temperatures, dew point, wind, and cloud cover. The soil moisture budget subroutine needs only 24-hour precipitation and 24-hour potential evapotranspiration (ETP) obtained from the heat budget subroutine by summing the four six-hour ETP calculations. Six-hourly observations are available only at first-order meteorological stations. Both the Manhattan, Kansas area and the Fargo, N.D. area have only one first-order station. These are Concordia for Kansas, and Fargo for North Dakota. Cooperative climatological stations, which provide the bulk of the meteorological data, have only maximum and minimum temperatures and daily precipitation. We therefore used the maximum and minimum temperatures to estimate six-hourly temperatures by assuming that the maximum temperature occurred at 3 PM local time and that the minimum temperature occurred at 6 AM local time. Temperatures were

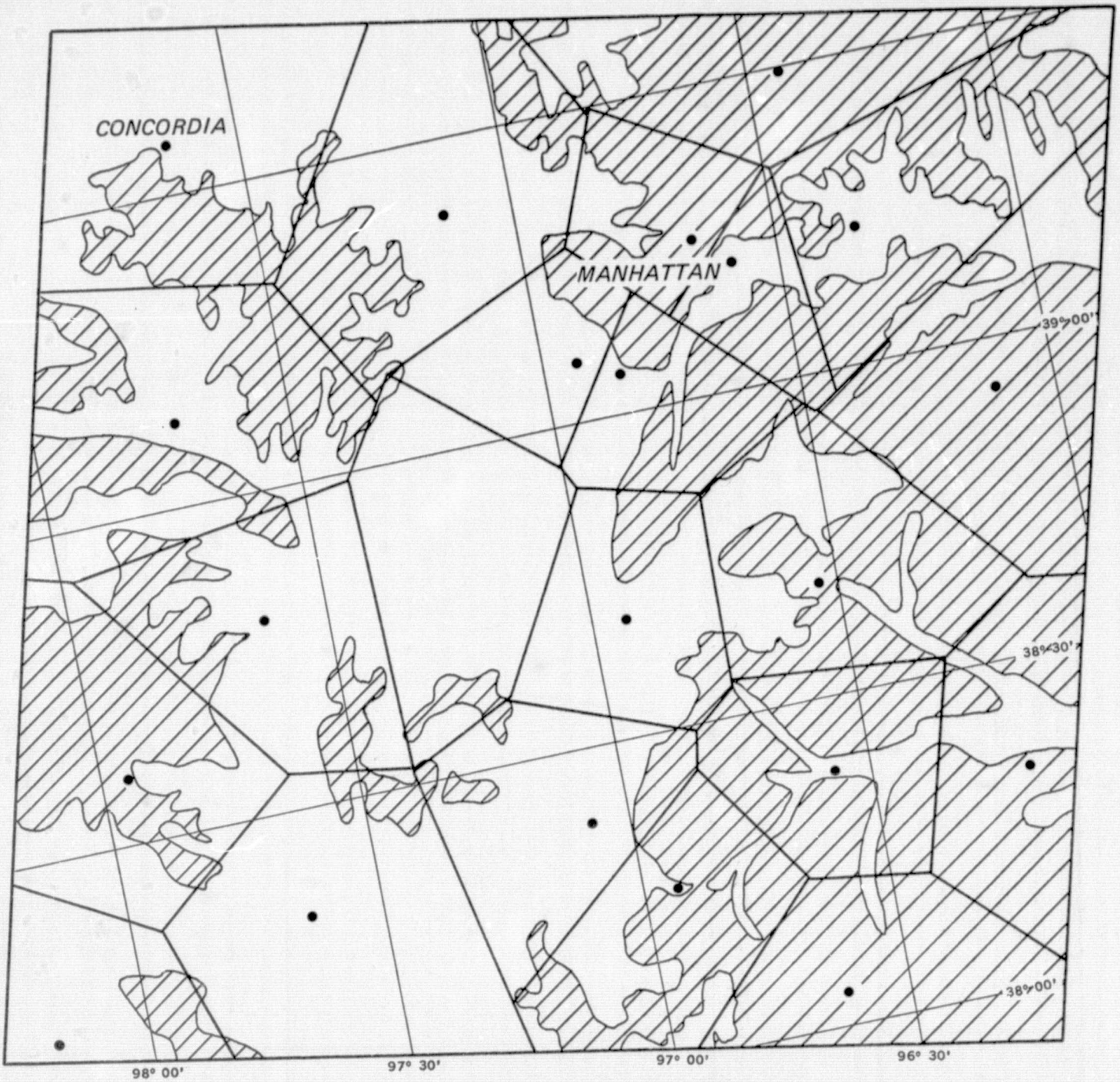

Figure 2-6: Generalized land-use map of the Manhattan, Kansas area derived from Landsat MSS images (adapted from Williams and Barker, 1974). The dashed-in areas are mostly rangeland, the rest are mostly cropland. Dots show location of climatic stations used for the surface heat and moisture budget calculations for the period 18-24 May 1974. A polygon around each station defines the station's area of influence for the purpose of the budget calculations.

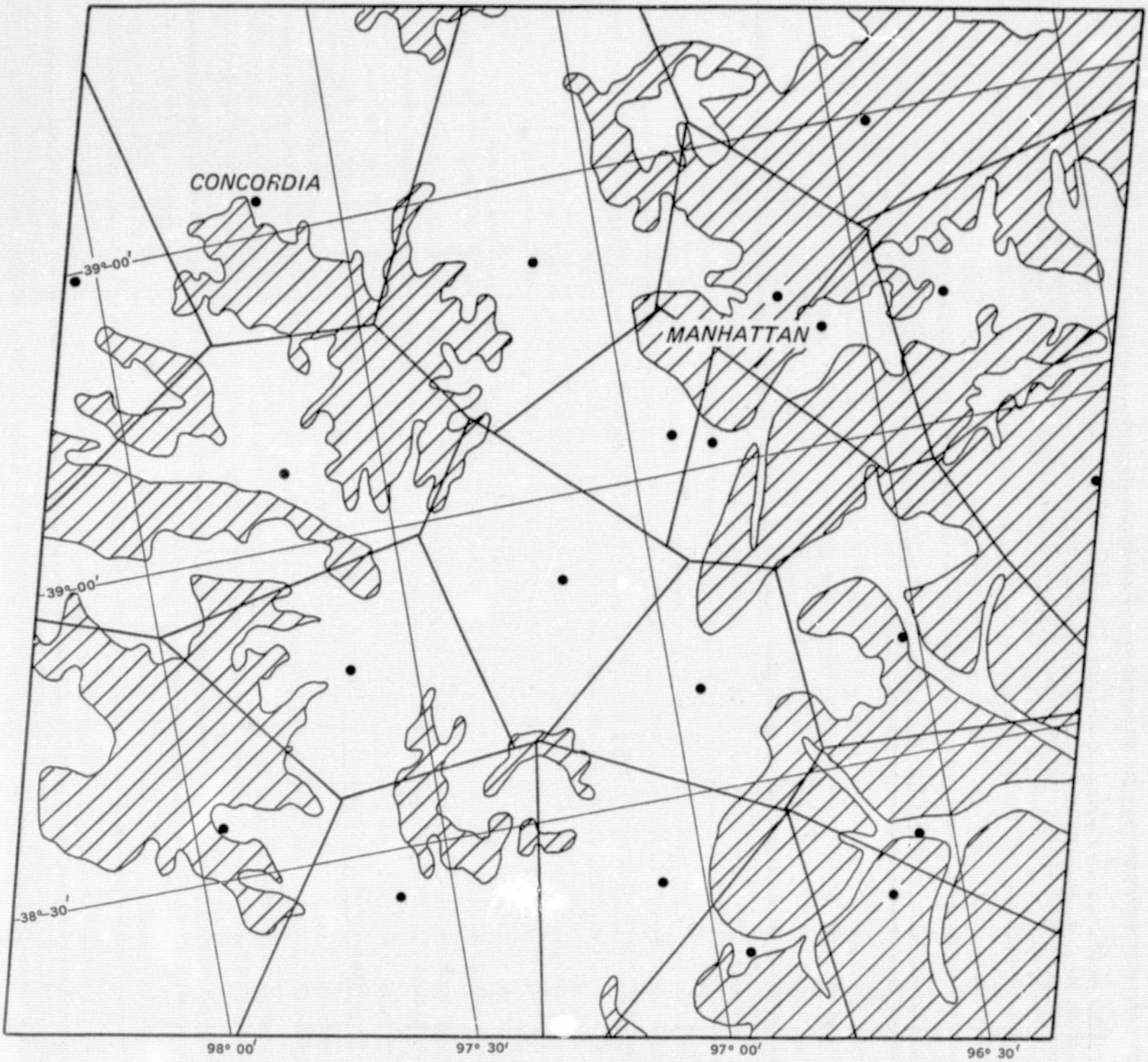

Figure 2-7: Generalized land-use map of the Manhattan, Kansas area derived from Landsat images (adapted from Williams and Barker, 1974). The dashed-in areas are mostly rangeland, the rest are mostly cropland. Dots show location of climatic stations used for the surface heat and moisture budget for the period 15 June - 3 July 1975. A polygon around each station defines the station's area of influence for the purpose of the budget calculations.

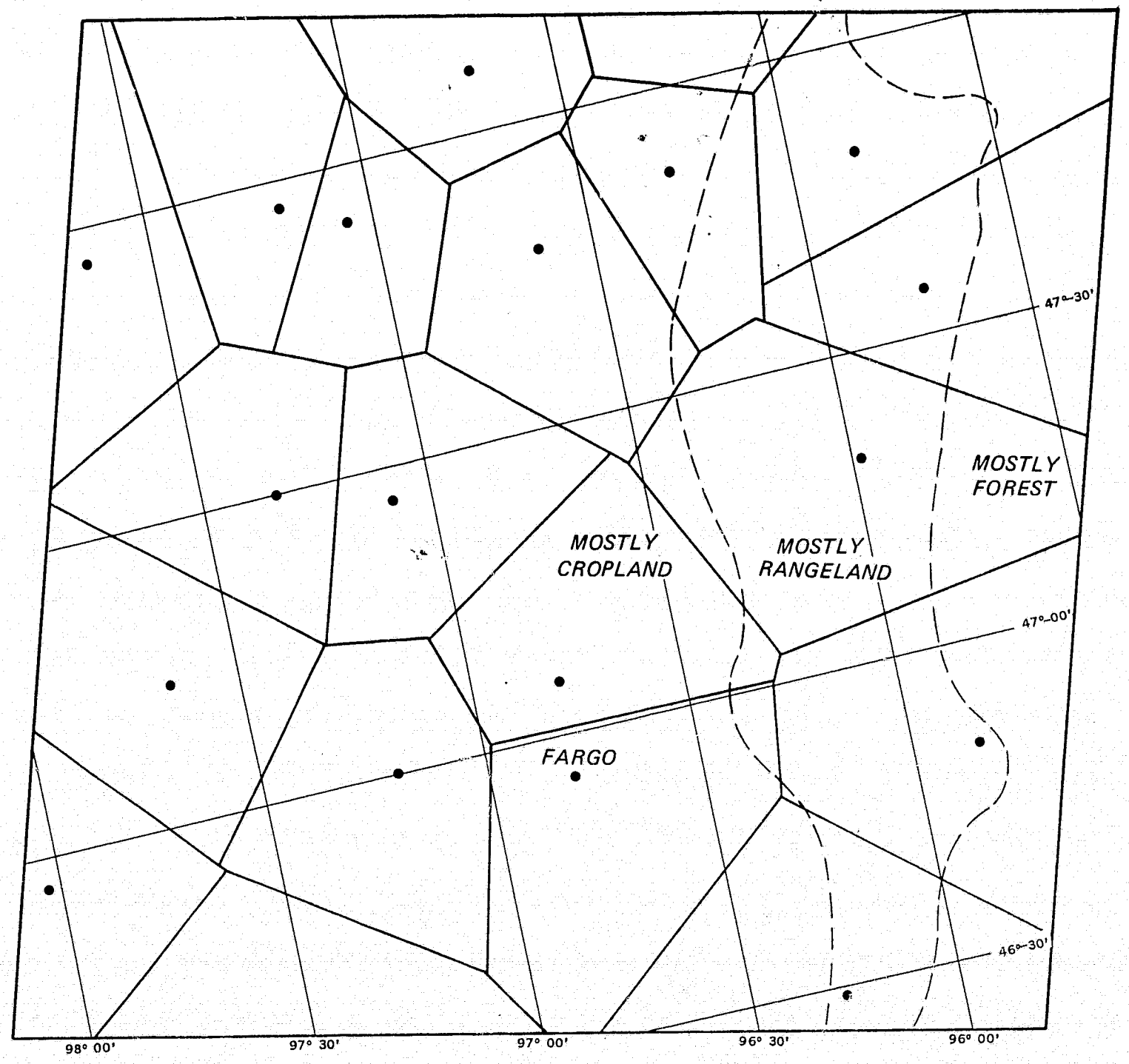

Figure 2-8: Generalized land-use map of the Fargo, North Dakota area derived from the Landsat-2 MSS color composite image of 5 July, 1975 (not shown). Dots show location of climatic stations used for the surface heat and moisture budget calculations for the period 28 June - 5 July 1975. A polygon around each station defines the station's area of influence for the purpose of the budget calculations.

estimated by linear interpolation at 3, 9, 15, 21 GMT, which are the midpoints of the four six-hour intervals used for our heat budget calculations (0-6, 6-12, 12-18, 18-24 GMT). Six-hourly dew point temperatures, wind, and cloud cover from the first-order stations were then used to complete the needed data for the heat budget calculations.

The climatological data from the first-order stations and co-operative observers' stations were punched on computer cards. Data were collected for about one to two weeks prior to the selected Landsat images, to insure that the budget calculations would be started far enough in time to include a few widespread precipitation events which would cancel any inaccuracy in the soil moisture starting conditions. The method for calculating the heat and soil moisture budgets will be detailed in Section 3.

2.4 Atmospheric Soundings

In order to compare the values of the heat available for heating air obtained from our budget calculation to the energy needed for free convection we analyzed atmospheric soundings from stations in or near our areas of interest. Soundings taken in the mornings of the three selected Landsat images were obtained from the National Climatic Center, Asheville, N.C. The soundings were taken at about 1115 GMT, while Landsat passed at about 1630 GMT. For the two Manhattan cases we received soundings for Omaha, Nebraska; Dodge City, Kansas; and Topeka, Kansas. For the Fargo case we received soundings from Bismarck, N.D. and International Falls, Minnesota. Results of these analyses will be presented in Section 3.3.

3.0 CALCULATION OF HEAT AND MOISTURE BUDGETS

This section describes the physical model employed in the calculation of heat and moisture budgets for the climatological sites within the Landsat image area.

The problem is to determine how much sensible heat has been contributed by the ground to the atmosphere in the daylight hours prior to the time of the Landsat image (approximately 10 AM local solar time). This sensible heat would then be responsible for heating the air near the surface and therefore setting off convective currents which would manifest themselves in the appearance of cumulus clouds at the condensation level. The model aims at describing what happens to the radiant energy and moisture contributed to the ground by the sun and rain.

The main features are:

1. A radiation and energy subroutine which calculates net radiation (R_{NET}) and potential evaporation (ETP) from surface temperature, dew point, wind, cloud cover, albedo, and earth-sun geometry; and
2. A soil moisture budget subroutine which estimates moisture in three ground layers and actual evaporation (ET) to the atmosphere from precipitation, ETP, soil type, and plant cover root structure.

The energy available to heat the air near the surface (from sunrise to the time of Landsat image) can be estimated by considering the following simplified form of the surface heat budget equation:

$$R_{NET} - E = L \qquad (3.1)$$

where

L is the heat exchanged from surface to air;

R_{NET} is the radiation balance (difference between incoming solar and outgoing terrestrial radiation); and

E is the heat used in evaporation.

Equation 3.1 is a gross over-simplification of what really happens in nature. It neglects heat flow from or to the subsurface, heat transport by horizontal air movement, or heat used in photo chemical processes taking place in the plant cover. Equation 3.1 simply states that L, the portion of the radiation balance left after evaporation, is available to heat the air.

Actual evaporation taking place the morning of the Landsat image is determined by how much moisture is available near the surface; it is therefore necessary to begin the moisture and heat budget calculation some time before, preferably at a time when surface moisture starting conditions are known. The start time for each of the three cases considered was chosen to be just before a widespread rainfall event, assuring the soil moisture to be near or above 50% of capacity after the rainfall.

The inputs, intermediate outputs, and final outputs of the heat and moisture budget models are diagrammatically illustrated in Figure 3-1a, b. The following subsections detail the methodology in the calculation of the various parameters necessary for the heat and moisture budgets. Since surface albedo is one of the important parameters governing R_{NET} and is obtained directly from the Landsat images, we shall start with a description of how albedo is estimated.

3.1 Albedo Calculations from Landsat Radiances

The surface albedo A, defined as the ratio of outgoing to incoming solar radiation, was estimated by the following equation:

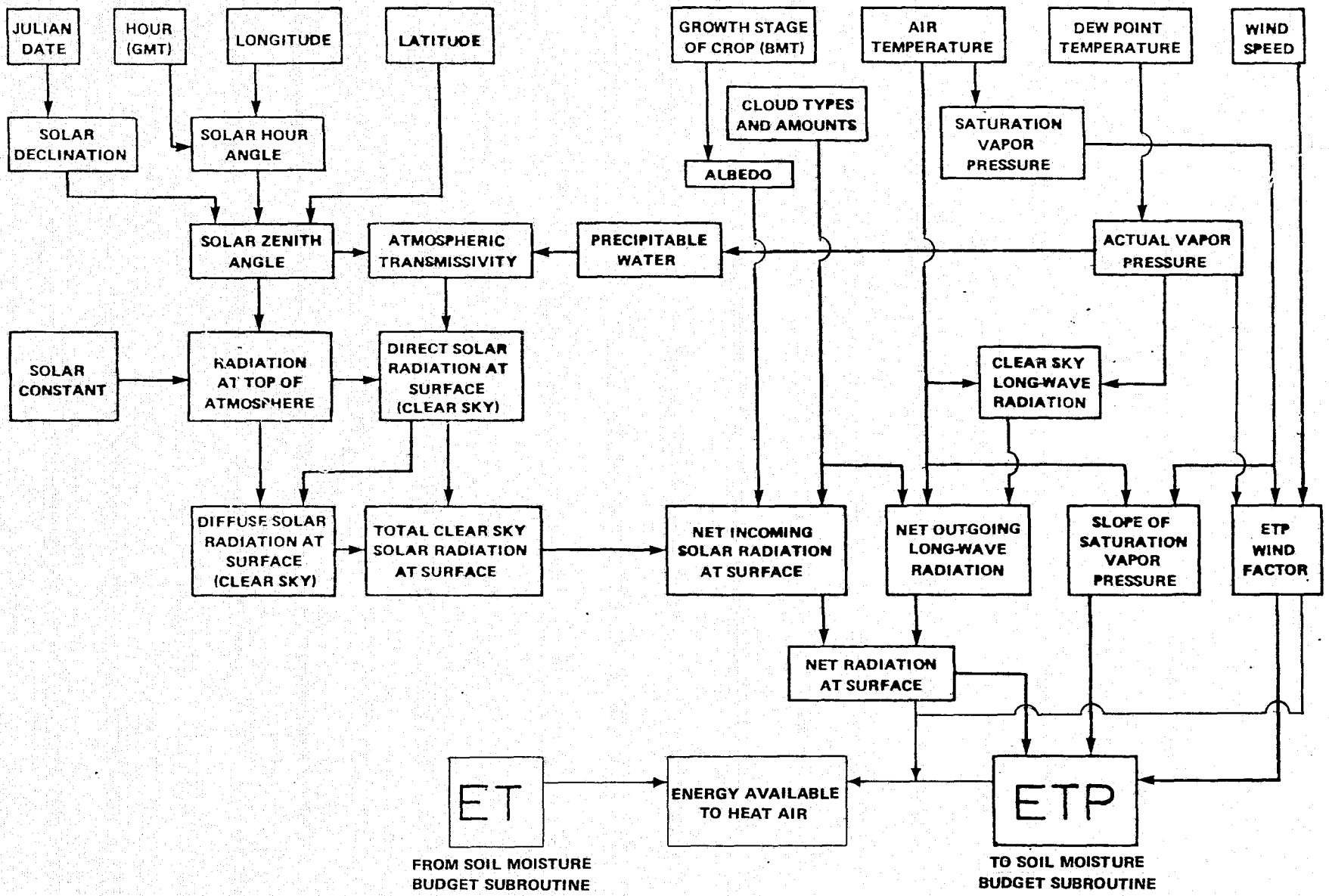

Figure 3-1a: Schematic diagram of Radiation Subroutine showing parameters involved in the calculation of evapotranspiration (ETP) by the Penman method, net radiation, and energy available to heat air. After calculation of net radiation and ETP control is transferred to the Soil Moisture Budget subroutine (Figure 3-1b) for the calculation of evaporation (ET).

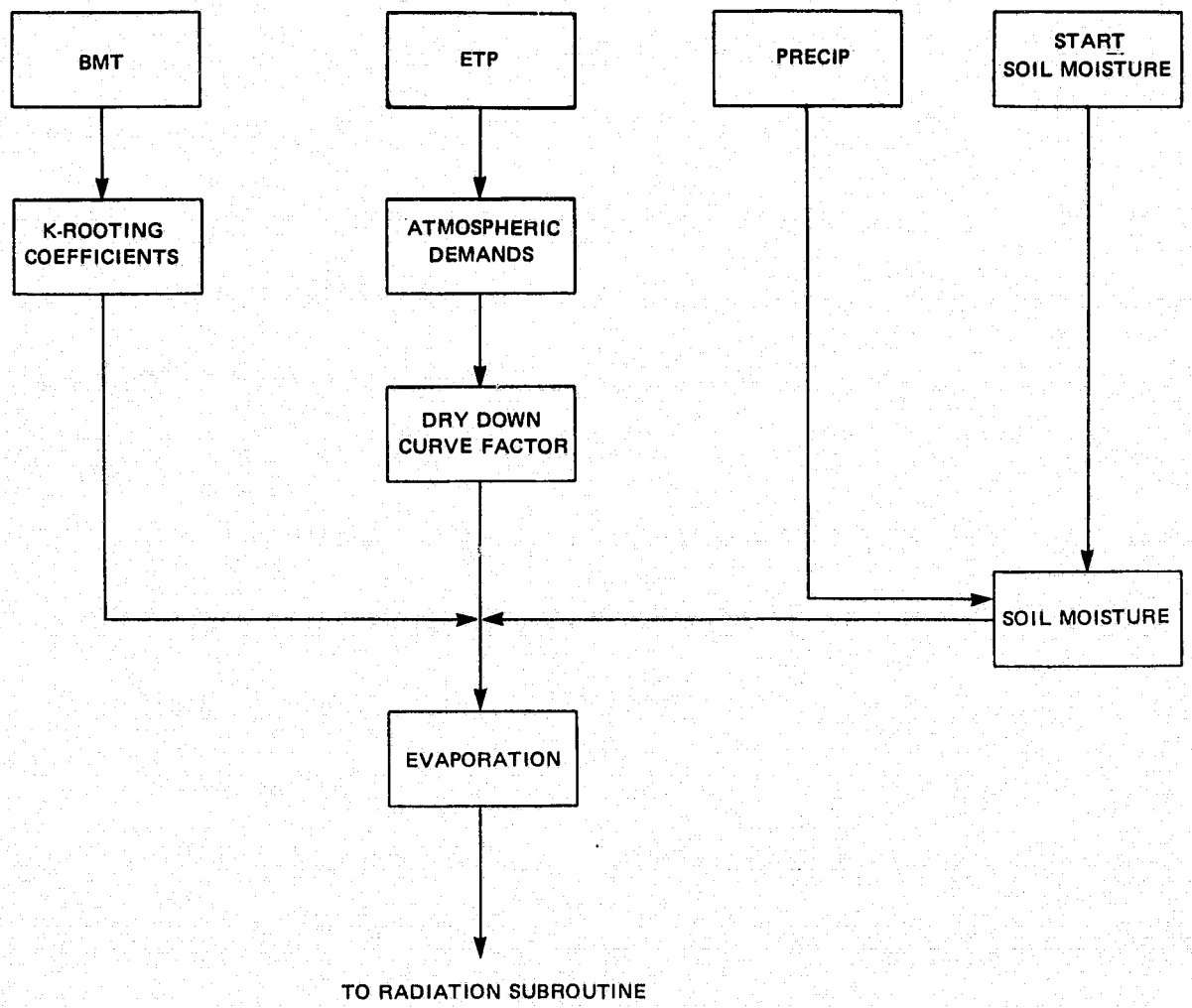

Figure 3-1b: Schematic diagram of Soil Moisture Subroutine showing parameters involved in the calculation of evaporation (ET). After calculation of ET control is transferred to the Radiation Subroutine (Figure 3-1a) for the calculation of energy available to heat air.

$$A_{0.5\text{-}1.1} = \frac{\pi}{\cos\theta} \quad \frac{\Sigma\,(N_i - S_{i\uparrow})/T_i\,(Z)}{\Sigma\,(H_i T_i(\theta)) + \Sigma S_{i\downarrow}} \qquad (3.2)$$

where

N_i ($i = 1,2,3,4$) are radiances measured by the four MSS bands;

$S_{i\uparrow}$, $S_{i\downarrow}$ are scattered atmospheric radiation to space and to the earth's surface estimated for each of the four MSS bands;

$T_i(Z)$, $T_i(\theta)$ are the average transmittances in the zenith and at solar zenith angle θ for each of the four MSS bands;

H_i are the integrated solar spectral radiances at the top of the atmosphere.

The surface albedo obtained by equation 3.2 is an estimate because we are considering only that part of the spectrum sensed by the MSS channels (0.5 - 1.1μm). Table 3-1 shows the solar radiances at the top of the atmosphere and the percentages of the total solar radiance within each MSS spectral band at the top of the atmosphere and received at the surface at a solar zenith angle of 60°. Since the MSS spectral bands measure almost two-thirds of the total reflected solar radiance from the ground and atmosphere, we may assume that the albedo calculated by equation 3.2 is a good approximation to the true albedo. Values of scattered radiance to space $S_{i\uparrow}$ in each of the four MSS bands were taken from Malila et al. (1975). These are shown in Table 3-2. The scattered component of the solar radiation to the earth's surface was estimated by using the ratio between the direct solar radiation and total solar radiation given by the Smithsonian Meteorological Tables (Table 150, p. 439). This

TABLE 3-1

Solar Radiation at Top of Atmosphere and Received at Surface in MSS Bands

Band	Spectral Interval (μm)	% Solar Radiation* Outside of Atmosphere (Zenith)	Solar Radiation** at surface (60° Zenith)	Solar Radiation* At top of Atmosphere (mw cm^{-2})
1	0.5-0.6	13.7	16.0	19.3
2	0.6-0.7	11.6	15.4	16.2
3	0.7-0.8	9.1	12.4	12.7
4	0.8-1.1	17.8	24.0	24.6
Totals		52.2	67.8	72.8

* Calculated from the Smithsonian Meteorological Tables (1966)

** Calculated from Moon (1946) assuming a standard atmosphere

TABLE 3-2

Values of Scattered Radiance to Space, From Malila et al (1975)

Band	Spectral Interval μm	Radiance Counts	Scattered to Space Radiance (mw $cm^{-2}sr^{-1}$)
1	0.5-0.6	14	.27
2	0.6-0.7	7.5	.12
3	0.7-0.8	6	.08
4	0.8-1.1	1.5	.11

ratio is 0.84 for the range of solar zenith angles of our three Landsat images (30°, 31°, 34°).

The atmospheric transmittances for the four MSS channels were calculated with the aid of Figures 3-2a and b. Table 3-3 shows the transmissions in the vertical and at the appropriate zenith angles for the four MSS channels for the three cases. In all three cases, we assumed a standard atmosphere and 2 cm of precipitable water.

Because of cloud cover shown by the 3 July 1975 and 24 May 1974 images, we used Landsat data taken 18 days earlier (6 May and 15 June) which were clear or mostly clear, to estimate surface albedo in cloudy areas. Figures 2-1 to 2-5 present the Landsat images used in the study. Portions of the corresponding albedo maps are shown in Figures 3-3 to 3-6.

Because of the enormous amount of data in the 185 x 185 km image (equivalent to 7,581,600 pixels for each image), average albedo values were obtained for approximately 3.4 km^2 by sampling every eighth spot horizontally and every sixth spot vertically for a total of 16 samples. Thus, the albedo values shown are averages of 16 albedoes within 3.4 km^2 (1 sq.m). Surface albedoes vary spatially from low values of two percent for water bodies to about seventeen to twenty-five percent for cultivated fields, cities, and rangeland.

Albedo variations are not as great as one would expect from simply looking at the MSS 5 image. The contrasts that one sees on individual channel images almost disappear when the entire image of the MSS is considered. The main reason is that low reflectance of vegetation in the visible is compensated by high reflectance in the infrared.

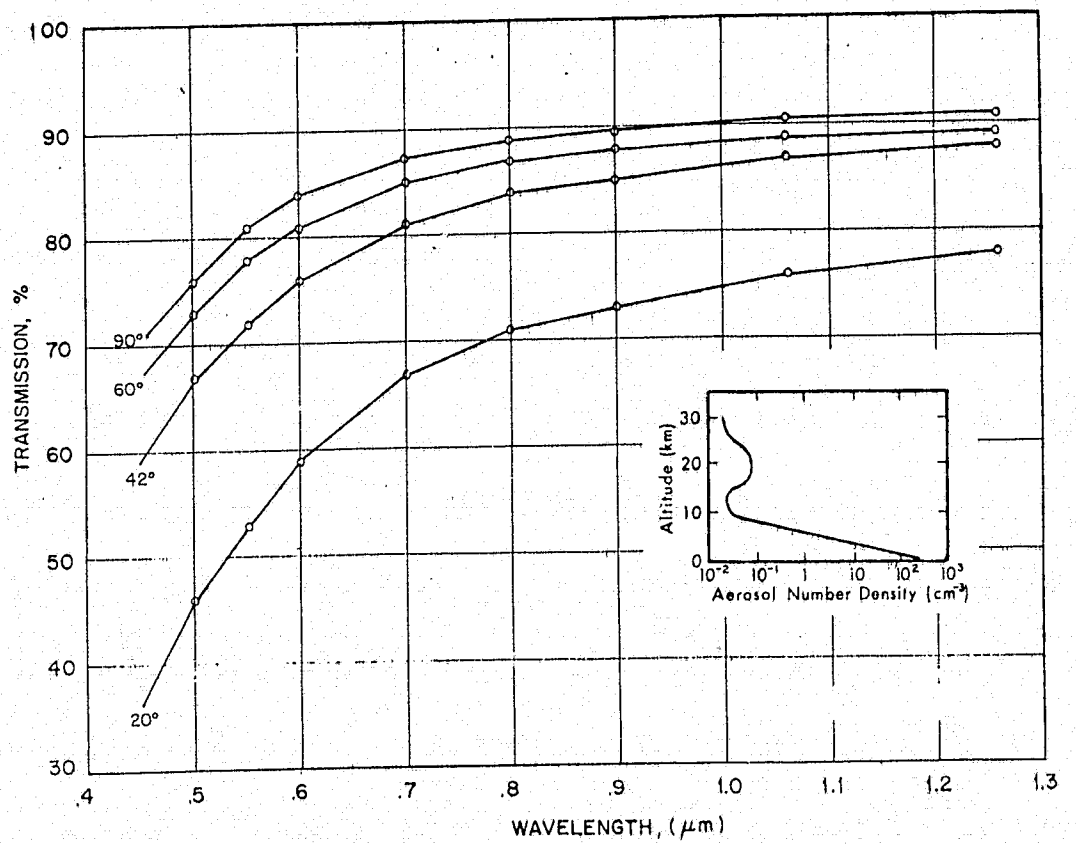

Figure 3-2a: Transmission for a dry turbid atmosphere at solar elevation angles of 90°, 60°, 42°, and 20° with aerosol distribution as shown and 0.229 cm of ozone. The graph, taken from Sabatini and Rabchevsky (1970), was constructed from transmission values tabulated by Elterman (1968).

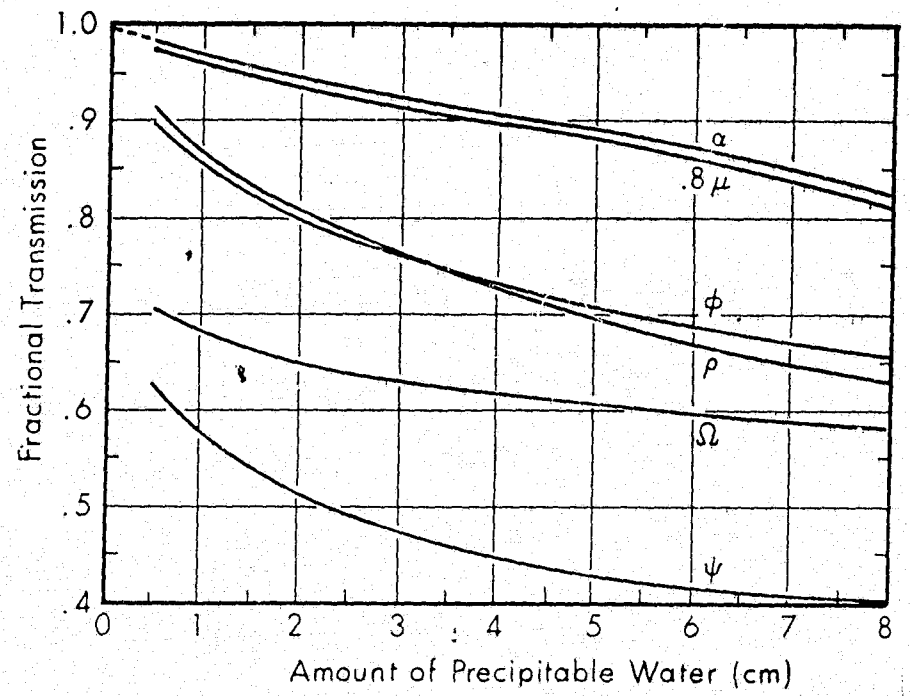

Band	Wave-length interval (μm)
α	0.70 - 0.74
.8μ	0.79 - 0.84
ρ	0.86 - 0.99
ϕ	1.03 - 1.23
Ω	1.24 - 1.53
ψ	1.53 - 2.10

Figure 3-2b: Transmission of solar radiation by water vapor (Smithsonian Meteorological Tables, 1966).

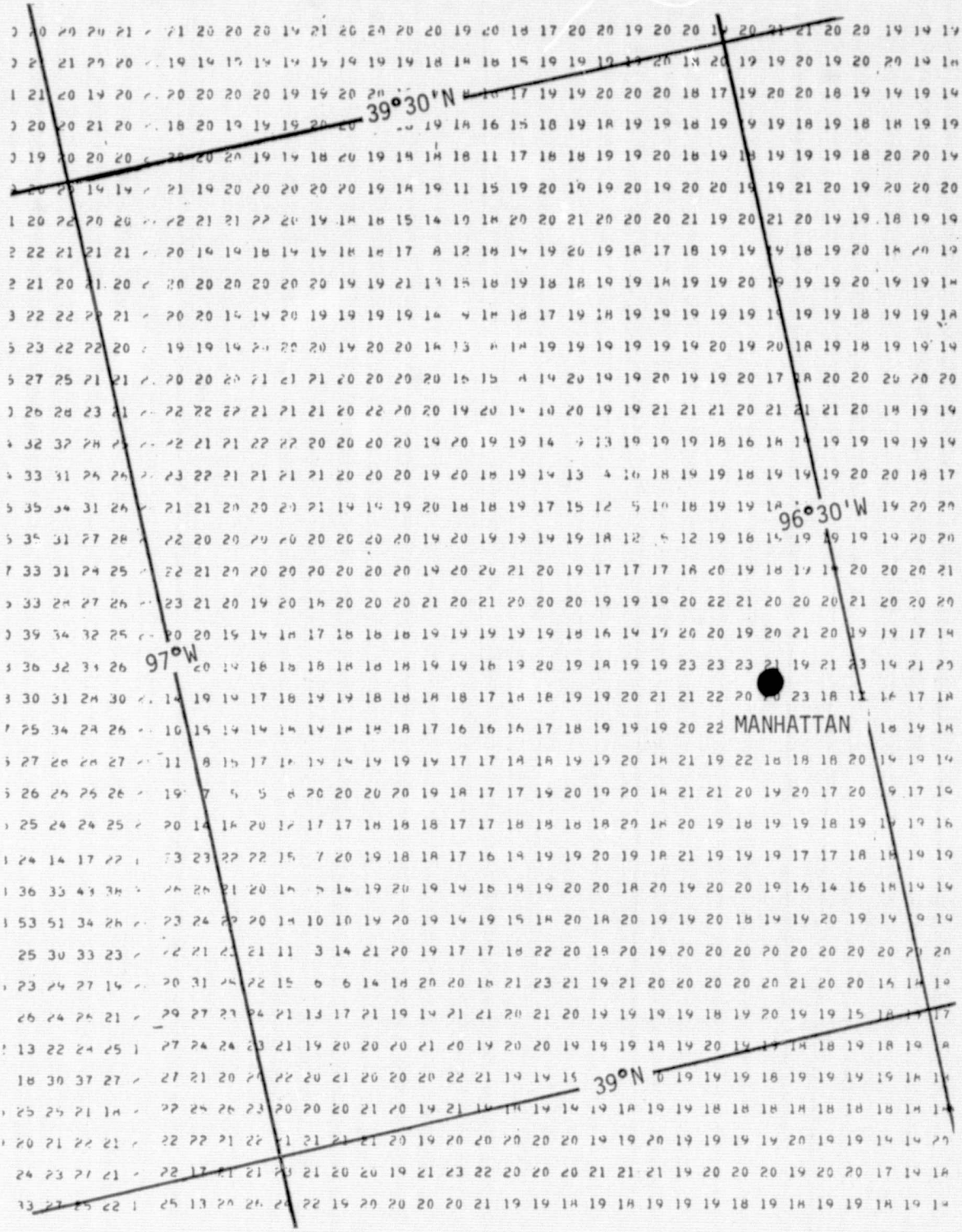

Figure 3-3: Albedo map for the Manhattan, Kansas area derived from the Landsat-1 MSS data taken on 6 May 1974 (see Figure 2-1). Albedo values in percentages are for 3.4 km^2 area.

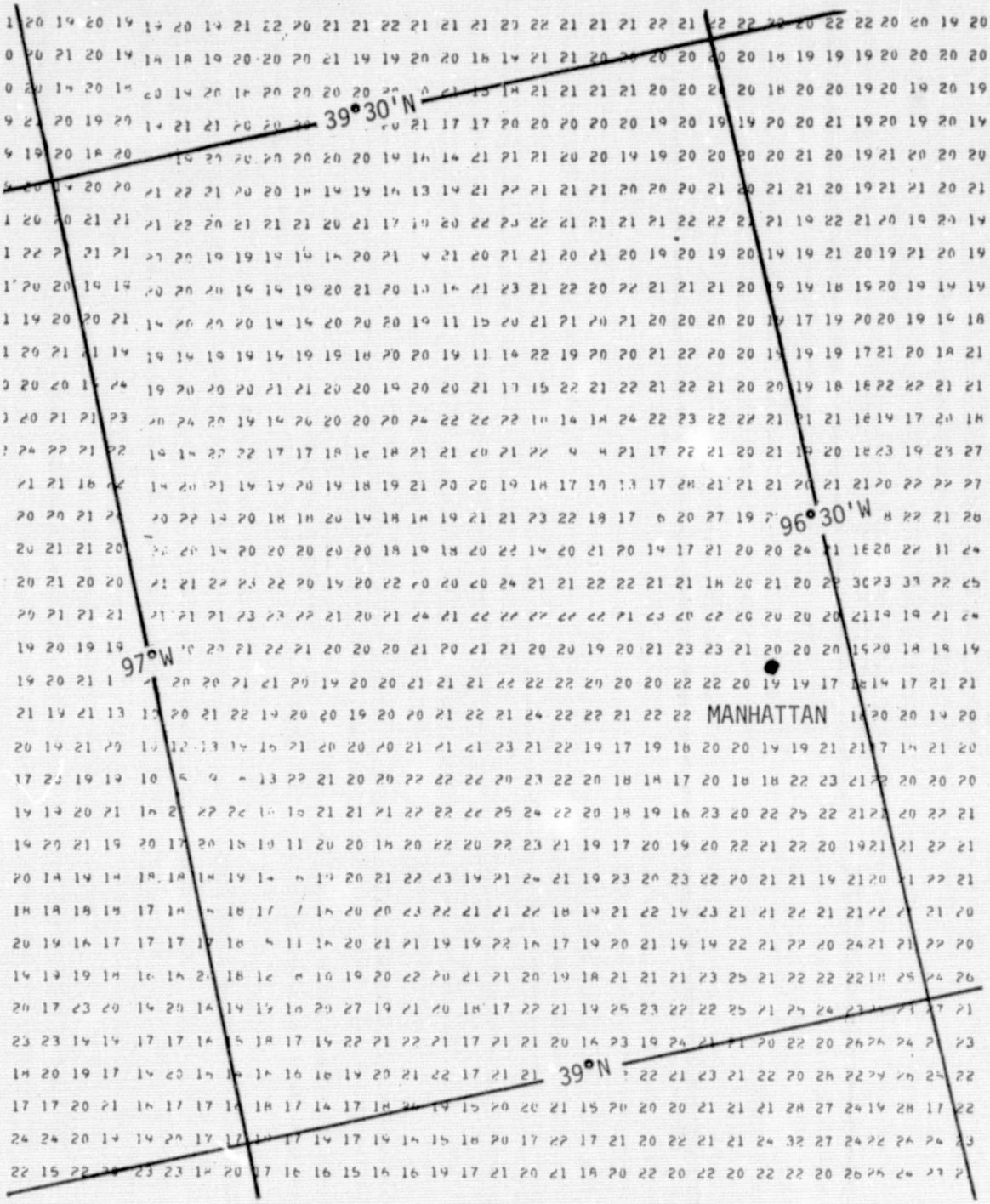

Figure 3-4: Albedo map for the Manhattan, Kansas area derived from the Landsat-1 MSS data taken on 24 May 1974 (see Figure 2-2).

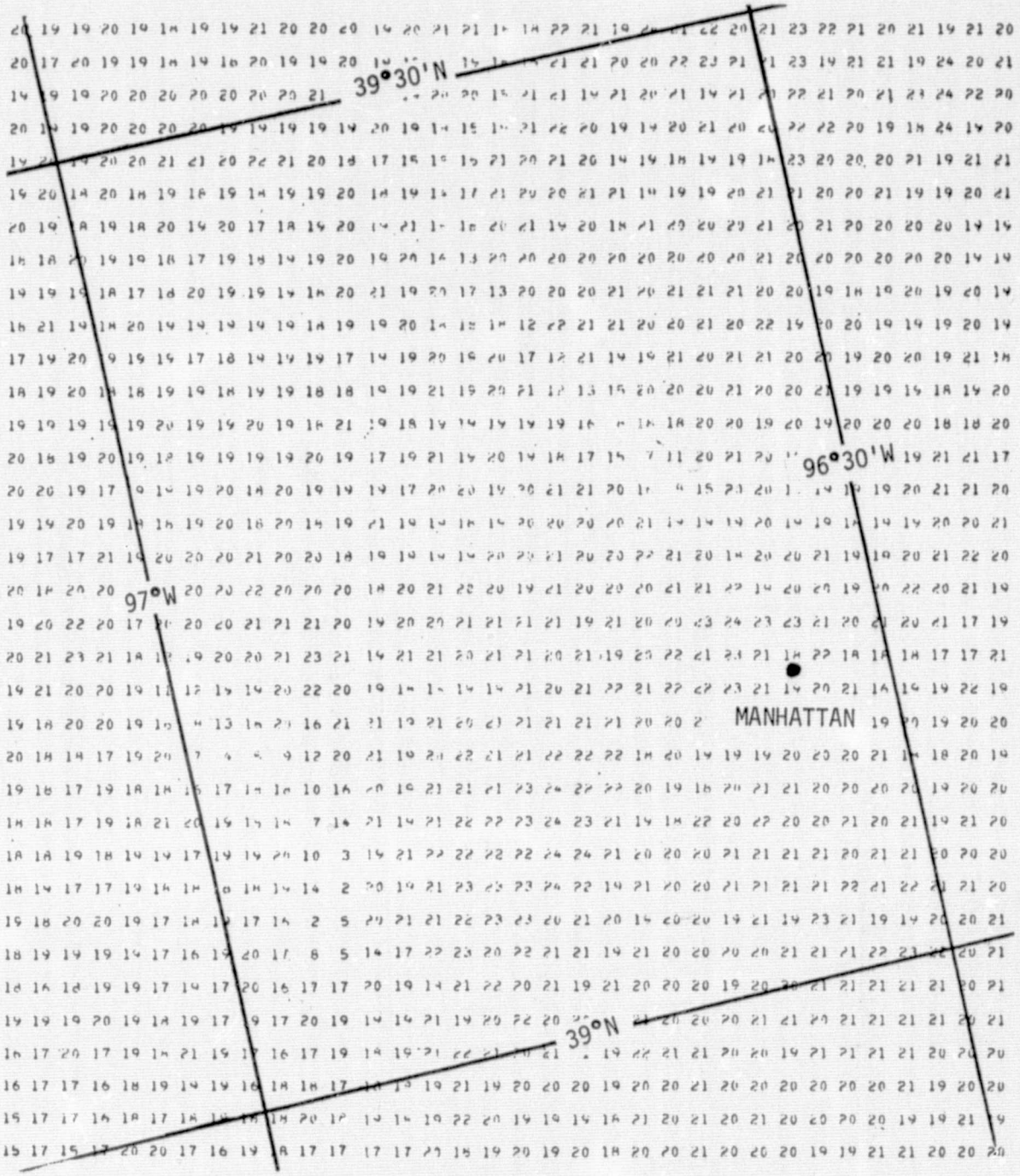

Figure 3-5: Albedo map for the Manhattan, Kansas area derived from the Landsat-2 MSS data taken on 15 June 1975 (see Figure 2-3).

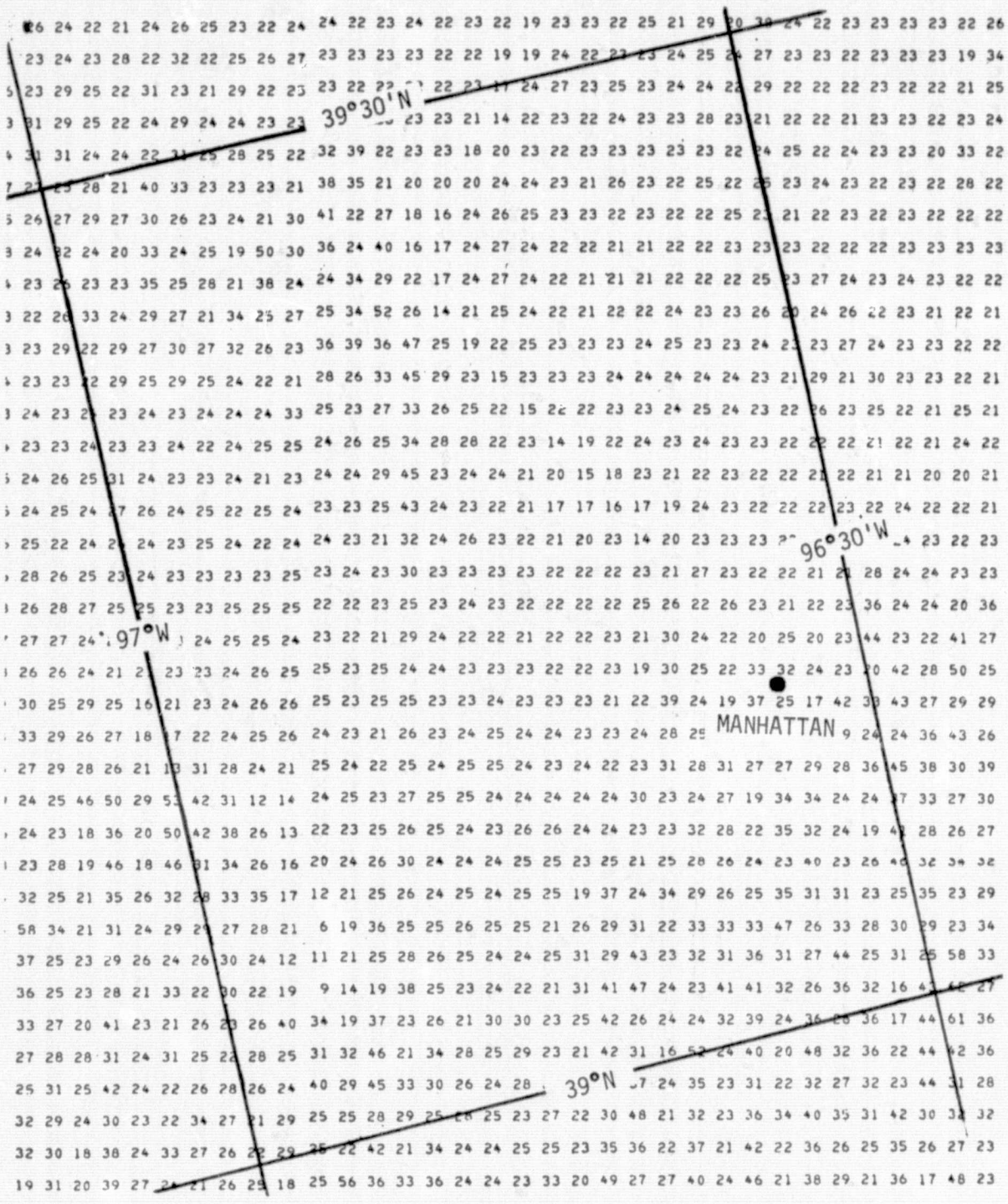

Figure 3-6: Albedo map for the Manhattan, Kansas area derived from the Landsat-2 MSS data taken on 3 July 1975 (see Figure 2-4).

Table 3-4 shows the average albedoes for the climatological stations for the two background images (May 6, 1974; June 15, 1975) and for the two images at the end of the budget calculations (May 24, 1974; July 3, 1975). The albedoes were estimated from the Landsat albedo maps (Figures 3-3 to 3-6) by averaging 16 values around each station when no clouds were present, but using only the lowest four values for partly cloudy conditions. Albedoes were found to vary only a few percentages in time and in space. We, therefore, decided to perform the heat and moisture budget calculations at each station using albedoes of fifteen, twenty, and twenty-five percent covering the range of observed surface albedoes. These calculations permitted us to estimate the relative importance of surface albedo in our heat and moisture budgets.

3.2 Heat and Soil Moisture Budget Calculations

The goal of the heat and soil moisture budget calculations is to determine how much heat, L, will be available for convection the morning of the Landsat image. L can be estimated, as Equation 3.1 shows, from a calculation of the net radiation at the surface R_{NET}, and the heat expended in evaporation, E. E is estimated from actual evaporation calculated by the Soil Moisture budget subroutine which keeps track of the moisture in the soil from inputs of potential evaporation (ETP), precipitation, and an assumed root structure. Figures 3-1a and b show the parameters involved in the ETP and soil moisture subroutine. ETP is calculated using the method of Penman (1947), and relies on estimation of net radiation. Computer subroutines to calculate R_{NET}, ETP, and ET have been adapted from the

TABLE 3-3

Atmospheric Transmittances for the MSS Bands
(Standard Atmospheric Conditions, 2 cm prec. water)

Band	Spectral Interval (μm)	T(Z) Vertical	T(θ) θ=30°
1	0.5-0.6	0.81	0.78
2	0.6-0.7	0.86	0.83
3	0.7-0.8	0.86	0.83
4	0.8-1.1	0.78	0.75

Values of atmospheric transmittances were estimated from Figures 3-2a, b. Solar zenith angles were 30°, 31°, and 33° for 24 May, 3 July, and 5 July Landsat images. No appreciable error is incurred in using the calculation for 30° zenith (60° elevation) for all three cases.

TABLE 3-4

Average Surface Albedoes Around Climatic Stations (4X4 miles)

Date	Average Albedo (%)	Standard Deviation	Number of Stations
May 6, 1974	20.2	1.2	20
May 24, 1974	20.4	1.4	21
June 15, 1975	19.9	1.0	21
July 3, 1975	22.7	1.4	10

EarthSat Spring Wheat Yield System (1976). The following subsections will explain how we calculate net radiation R_{NET}, potential evaporation ETP, and the heat expended in evaporation from the Soil Moisture Budget subroutine.

3.2.1 Net Radiation

Net radiation (R_{NET}) is the net energy gained by the surface through the processes of insolation and terrestrial radiation losses to space. R_{NET} is a measure of how much energy is available for heating the ground, and most importantly, for evaporation. R_{NET} is estimated by means of a combination of surface reports of temperature, dew point, and cloud cover.

The net radiation at the surface, R_{NET} (cal/cm^2), is the difference between the net solar radiation, R_{SN}, and the net long wave or terrestrial radiation, R_{LN}:

$$R_{NET} = R_{SN} - R_{LN}$$

Net solar radiation, R_{SN}, is that portion of the total incoming clear-sky solar radiation, $R_{sc}\downarrow$, not attenuated by clouds and not reflected by the earth's surface:

$$R_{SN} = (1 - A) F_s R_{sc}\downarrow$$

where A is surface albedo expressed as a decimal from 0 to 1.

F_s is a solar radiation cloud factor which is a function of cloud type and amount;

$R_{sc\downarrow}$ is the total incoming clear-sky solar radiation which is the sum of direct clear-sky solar radiation at the earth's surface, $R_{s\downarrow}$, and the diffuse solar radiation, R_d: $R_{sc\downarrow} = R_{s\downarrow} + R_{d\downarrow}$

The solar radiation cloud factors, F_s, were estimated with the aid of values of transmission of solar radiation through clouds (overcast) presented in the Smithsonian Meteorological Tables (1966), p. 441, and are presented in Table 3-5.

The formula used to estimate cloud factor for any given cloud condition is:

$$F_s = \Sigma\, n_t \cdot F_t + 1.0 - \Sigma\, n_t$$

where n_t is fraction of given cloud types, and F_t is overcast cloud factor for given cloud types as shown in Table 3-5.

The total incoming clear-sky solar radiation was estimated by a method developed by Klein (1948) and based on Kimball's charts of transmission of solar radiation (SMT, Table 147). For ease of computer calculations we translated Kimball's charts into polynomials. Transmission is then calculated as a function of air mass and total atmospheric water vapor.

The net long wave radiation, R_{LN} (cal/cm^2), is that portion of the long wave radiation that is lost to space:

TABLE 3-5

Solar Radiation Cloud Factors For Overcast Conditions
(Adapted from the Smithsonian Meteorological Tables, 1966)

Cloud Type	Cloud Factor, F_t
Cirrus (Ci)	0.84
Cirrostratus (Cs)	0.81
Altocumulus (Ac)	0.51
Oltostratus (As)	0.41
Stratocumulus (Sc)	0.34
Status (St)	0.25
Nimbostratus (Ns)	0.15
Fog	0.17

$$R_{LN} = R_{LC}^{\uparrow} - F_L \, (\sigma \, T_a^4 - R_{LC}^{\uparrow})$$

where $R_{LC}^{\uparrow}$ is the clear sky long wave radiation and is calculated by Geiger's method (1971):

$$R_{LC}^{\uparrow} = [\sigma \, T_a^4 \, (.18 + .25 \times 10^{-.065e}) - 0.007 \, (T_a - T_g)]$$

where T_a is air temperature

T_g is ground temperature ($T_g = T_a$ in our calculations)

$\sigma = 8.132 \times 10^{-11}$ cal/cm^2/min/deg^4

e is vapor pressure at air temperature

F_L is the long wave radiation cloud factor calculated for a combination of cloud cover and type by:

$$F_L = (\Sigma \sqrt{k_t \, W_t})^2$$

The above equation is a variant of the long wave cloud factor, kw^2, presented by Geiger (1971), which considers only one cloud type at a time. W_t is fraction of given cloud type, and k_t is a constant which depends on the cloud type. Values of k_t are as follows (Geiger, 1972): Ci, 0.04; Cs, 0.08; Ac, 0.17; As, 0.20; Cu, 0.20; St, 0.24.

Net radiation calculations are performed for six-hour intervals (0-6, 6-12, 12-18, 18-24 GMT). Six-hourly temperatures for 3, 9, 15, 21 GMT are estimated from the minimum and maximum temperatures at each climatic station by a linear interpolation and by assuming that minimum temperature occurs

at 6 AM Local Time and maximum temperature occurs at 3 PM Local Time. Since cooperative climatic stations do not report dew point or cloud cover, values of these parameters from the nearest first order station are used. Net radiation for the mornings of May 24 and July 3 was estimated with the assumption of no cloud cover.

3.2.2 ETP Calculations by the Penman Method

Evapotranspiration is the process by which water is transferred from the earth's surface to the atmosphere. It includes evaporation of liquid or solid water plus transpiration from plants. Potential evapotranspiration (ETP) is the amount of moisture which, if available, would be removed from a given land area by evapotranspiration, and is expressed in units of water depth. ETP is an input to our Soil Moisture Budget subroutine which estimates the actual evaporation.

The Penman equation for potential evapotranspiration is (Penman, 1948):

$$ETP\ (mm/time) = \frac{\Delta R_{NET} + 0.64\ f\ (w)\ (e_s - e_a)}{\Delta + 0.64} \qquad (3.3)$$

where

R_{NET} is net radiation in cal/cm^2 per time interval;

Δ is slope of saturation vapor pressure versus temperature curve ($mb\ °K^{-1}$);

e_s is saturation vapor pressure at air temperature (mb);

e_a is vapor pressure at air temperature (mb);

$f(w)$ is the wind effect, a function of the horizontal wind velocity.

The wind effect $f(w)$ is given by Penman (1956) as

$f(w) = 0.34\ (0.5 + w/100)$

where w is wind movement in miles per 24 hours.

The ETP calculations are performed for six-hour intervals at each climatic station in the area. The intervals are 0-6, 6-12, 12-18, 18-24 GMT. Daily ETP is obtained by summing up four six-hour calculations. For six-hour calculations the wind function becomes:

$$f(w) = 0.35\ (0.5 + 0.27618\ w)/4$$

where w is a surface wind measurement, in knots, made during the six-hour interval.

e_s, e_a, and Δ are calculated from six-hourly temperatures and dew point estimations by means of psychometric equations presented in the Smithsonian Meteorological Tables (1966) (see pp. 350 and 372).

3.2.3 Soil Moisture Budget Calculations

The basic soil moisture budget used was developed by Baier and Robertson (1966). This so-called "Versatile Budget (VB)" divides the total soil moisture into several zones. Water is extracted simultaneously from different depths in the soil profile permeated by plant roots, as a function of the rate of potential evapotranspiration (ETP) and the available

soil moisture in each zone. The general equation for the Versatile Budget model for calculating daily actual evapotranspiration per zone is:

$$ET_i = \sum_{j=1}^{n} k_j \frac{S'_j(i-1)}{S_j} Z_j \, ETP_i e^{-0.01w(ETP_i - \overline{ETP})} \quad (3.4)$$

where

ET_i = actual evapotranspiration for day i ending at the morning observation of day i + 1;

$\sum_{j=1}^{n}$ = summation carried out from soil zone 1 to N;

k_j = coefficient which account for soil and plant characteristics in the jth zone;

$S'_j(i-1)$ = available soil moisture in the jth zone at the end of day i-1, that is, at the morning observation of day i;

S_j = capacity for available water in the jth zone;

Z_j = adjustment factor for different types of soil dryness curves;

ETP_i = potential evapotranspiration for day i;

w = adjustment function accounting for effects of varying PE rates on the actual to potential evapotranspiration rate;

$\overline{ETP}$ = long-term average daily PE for month or season.

The term $e^{-0.01w\,(ETP_i - \overline{ETP})}$ accounts for effects of varying daily atmospheric demand rates (ETP_i) on the actual to potential evaporation rate as a function of available soil moisture. This term is set to unity whenever $ETP_i < \overline{ETP}$, and for estimating ET for a period less than a day. For an error

analysis of equation 3.4 the reader is referred to the EarthSat Spring Wheat Yield System Test 1975. Final Report (Earth Satellite Corporation, 1976).

The total volume of plant-available soil moisture in the soil profile is subdivided into three zones of varying capacities. The subdivision into zones and the amount of moisture held in each zone are arbitrary, but three "standard zones" have been adopted and contain respectively 5, 20, 75% of the total plant-available moisture in the soil profile. Because the root distribution differs in depth from soil to soil, the location of the zones also differs but not the fractional subdivision of the total available soil moisture. The adaptation of standard zones makes it possible to use one set of crop coefficients for a particular crop in any type of soil, because it is assumed that the uptake of available water by crops always follows a characteristic pattern that depends on plant rooting habits.

Crop coefficients (k) express the amount of water as a fraction of ETP that is extracted by plant roots from the different zones during the growing season. To simulate this water uptake, the k-coefficients change during the growing season according to crop-developing stages or on a biometeorological time (BMT) scale basis.

The soil budget subroutine was originally implemented for spring wheat, with the k-coefficients reflecting the growth of spring wheat roots. For the purpose of our soil budget analysis which for our three cases is over an area of perennial prairie grass and fields cultivated with mostly wheat and corn, we have run the model assuming three sit-

uations: one with the rooting coefficients for spring wheat and a biometeorological time (BMT) reflecting the stage of growth of wheat, another with the rooting coefficients for sod grass and an appropriate estimated BMT, and a third situation with bare or fallow ground. The Fargo, N.D. area contains mostly wheat fields and inundated sugar beet fields. For this third case we have only run the Budget for the wheat situation, and for bare ground. The BMT and k-coefficient values were estimated from those given by Baier et al (1972) but modified for our three-layer soil model. Additionally, we assumed a loam soil with a full-field capacity of 175mm of water distributed five, twenty, and seventy-five percent in each of the three soil layers starting from the top layer. The soil moisture subroutine was started at fifty percent full capacity eight days before the May 24 case, and 13 days before the July 3 case. The 5 July 1975 case occurred in an area and during a time in which the EarthSat Spring Wheat Yield System (EarthSat, 1976) was operative. We therefore used for starting conditions the soil moisture values estimated by this system on 28 June 1975, the start time of our budget calculation for the 5 July case. The average BMT values for this area and for the time intervals of 28 June - 5 July 1975 were also obtained from the EarthSat Spring Wheat Yield System. These soil moisture starting conditions and times were chosen to insure that the budget would quickly reach a stable level after a few days by the inclusion of a few good widespread precipitation events during the period. Table 3-6 summarizes the starting conditions.

In our analysis, the soil moisture budget is calculated for each full day except for the day of the Landsat images (24

TABLE 3-6

Biometeorological Times, K-coefficients, and starting soil moisture used in the Moisture Budget calculations

	MAY 18-24, 1974	June 15-July 3, 1975	June 28-July 5, 1975
BMT - fallow	-1	-1	-1
BMT - wheat	2.7	4.8	2.7
BMT - grass	1	3	-
K - coeff - wheat	0.4, 0.4, 0.25	0.4, 0.5, .25	0.4, 0.4, 0.25
K - coeff - grass	0.5, 0.35, 0.15	0.5, 0.35, 0.15	-
K - coeff - fallow	0.4, 0.27, 0.13	0.4, 0.27, 0.13	0.4, 0.27, 0.13
Start soil moisture (mm)	4, 18, 65	4, 18, 65	8, 31, 118

May, 3 July, 5 July) at which times the calculations are performed only up to the times of the Landsat images.

3.2.4 Estimation of Heat Available for Convection

In our simple surface heat budget equation the heat available for convection is what is left over from the net radiation after some of this net radiation is spent on evaporation. Since potential evaporation, ETP (and therefore evaporation, ET) is composed of a wind effect and a net radiation effect, we are concerned only in that fraction of ET due to net radiation. The Penman equation for ETP can be re-written as:

$$ETP = \frac{\Delta \cdot R_{NET}}{\Delta + 0.64} + \frac{0.64\, f(w)\, (e_s - e_a)}{\Delta + 0.64}$$

where the first term on the right is the ETP due to net radiation, and the second term is the ETP due to wind. Since the actual evaporation ET as estimated by the soil moisture budget subroutine depends on ETP, we have assumed that the fraction of ET due to net radiation is the same as the fraction of ETP due to net radiation. This fraction is simply:

$$F_{NET} = 1 - \frac{ETP(wind)}{ETP}$$

where ETP(wind) is the ETP due to wind, and is the second term in the previous equation. The heat L available for convection is therefore:

$$L = R_{NET} - (ET) \cdot (F_{NET}) \cdot 58.6 \text{ calories}$$

where ET is the actual evaporation in mm taking place the morning of the Landsat image and calculated by the soil moisture budget subroutine, and 58.6 are the calories per cm^2 required to evaporate one mm of water.

3.2.5 Estimation of Heat Needed for Convection from Atmospheric Soundings

Heat from the ground is carried to the atmosphere by mixing of the lower layers due to friction and convection. Frictional exchange is caused by turbulent air flow over rough surfaces and is usually characterized by small cloud parcels randomly distributed. Even the smoothest vegetation surfaces provide sufficient roughness to cause turbulent flow (Geiger, 1971). Convective mixing occurs when the layer near the ground is heated above the adiabatic temperature lapse rate. Convective parcels are larger than frictional parcels and usually have a symmetrical distribution. Having overcome the adiabatic lapse rate, buoyant overheated parcels of air rise and colder air sinks to take their place. Convection resolves itself into patterns of ascending and descending motions with clouds forming in the ascending air.

In the early morning mixing is at first entirely frictional, but as the sun's heating of the surface increases there may be a sudden transition to convective mixing. If the heat available from the surface exceeds that needed to heat the layer under the morning inversion to the adiabatic lapse rate, then free convection may begin and clouds may form at the condensation level, provided enough moisture is present in the rising air. We therefore analyzed atmospheric soundings

taken in and around the area of interest to determine (1) the amount of heat necessary to heat the layer under the morning inversion to the adiabatic lapse rate; and (2) the height at which cumuliform clouds would form.

Early morning soundings (approximately 0515 LST) of the day of the Landsat images were plotted in a SKEW-T LOG-P diagram to perform the analyses. We will call the height at which cumuliform clouds would form the convective condensation level (CCL), although our method of calculating the CCL is somewhat different from the method of meteorological textbooks.* From a plot of the soundings, we first determined the thickness of the inversion layer and assumed parcels in the layer will be heated to the adiabatic lapse rate, and therefore obtain enough buoyancy to be lifted to the convective condensation level (CCL). The CCL at which cumuliform clouds form is the intersection of the dry adiabat (from the surface potential temperature) and the mixing ratio from the surface dew point. Table 3-7 presents the heights of the CCL calculated from the atmospheric soundings.

The amount of heat necessary to heat the layer under the morning inversion to the adiabatic lapse rate is proportional to an area on the SKEW-T LOG-P diagram bounded by the atmospheric temperature curve, the potential temperature curve from the top of the inversion to the surface, and the surface pressure.

* The textbook CCL as defined by Saucier (1955) is the point of intersection of the temperature sounding curve with the saturation mixing ratio line corresponding to the average mixing ratio in a surface layer of approximately 500 meters thickness.

TABLE 3-7

Height of Condensation Level Calculated From
1115 GMT Soundings

May 24, 1974:

Station	Height (Meters)
Omaha, Nebraska	1600
Topeka, Kansas	1250
Dodge City, Kansas	1200

July 3, 1975:

Omaha, Nebraska	1200
Topeka, Kansas	1300
Dodge City, Kansas	800

July 5, 1975:

International Falls, Minnesota	1050
Bismarck, North Dakota	1300

The equation to estimate the amount of heat ΔH needed to initiate free convection (or to heat the air under the inversion to the adiabatic lapse rate) can be derived from the first law of thermodynamics, the equation of state of air, and the specific heat of air. The first law of thermodynamics is:

$$dh = du + pd\alpha \tag{3.5}$$

The equation of state in differential form is:

$$pd\alpha + \alpha dp = RdT \tag{3.6}$$

and the change of internal energy du of air is:

$$du = C_v\, dT \tag{3.7}$$

In the above equations:

p = pressure;

α = specific volume;

R = ideal gas constant;

T = temperature;

dh = heat gain or loss per unit mass;

du = change of internal energy of gas per unit mass;

$pd\alpha$ = work done on gas per unit mass;

C_v = specific heat of day air at constant volume.

Substituting equations (3.7) and (3.6) into (3.5) we obtain:

$$dh = (C_v + R)dT - \alpha dp$$

Considering the heating as isobaric (dp = 0) and substituting the specific heat of dry air at constant pressure $C_{pd} = C_v + R$, we obtain:

$$dh = C_{pd}\, dT$$

For moist air we obtain by analogy:

$$dh = C_{pm}\, dT \qquad (3.8)$$

where C_{pm} is specific heat of moist air at constant pressure,

For a column of air one cm^2 of pressure thickness ΔP, the total mass in grams is $\Delta P/g$, g being the acceleration of gravity. Multiplying both sides of (3.8) by this mass we have:

$$dh\,\frac{\Delta p}{g} = \Delta H = C_{pm}\,\Delta T\,\frac{\Delta p}{g} \qquad (3.9)$$

which is the equation we have used to calculate heat (in cal/cm^2) needed to heat a column of air to the adiabatic lapse rate.

In equation (3.9):

g = acceleration of gravity (cm/sec^2);

ΔH = heat added to air column (cal/cm^2);

ΔP = pressure interval of inversion layer ($dynes/cm^2$);

ΔT = potential temperature minus actual temperature in inversion layer (°K). Adiabatic lapse rate is

represented by constant potential temperature lines in a SKEW-T LOG-P diagram;

C_{pm} = specific heat of moist air at constant pressure (cal/g-K°).

C_{pm} is related to the specific heat of dry air C_{pd} by:

$$C_{pm} = C_{pd} (1 + 0.8Q)$$

where:

Q = mixing ratio, and

C_{pd} = 0.24 cal/g-K°

Δp and ΔT are obtained from analysis of the soundings plotted on the SKEW-T LOG-P diagrams. ΔT represents the difference between the surface temperature and the potential temperature brought down from the top of inversion. ΔP represents the pressure difference between the top of the inversion and the surface.

The results of the analysis are given in Table 3-8.

3.3 Results of the Heat and Soil Moisture Budget Calculations

The distribution of cultivated land and rangeland shown in Figures 2-6 to 2-8, the Landsat albedo maps, and the meteorological observations at the climatic stations, were all utilized for conducting the heat and soil moisture budget calculations.

At each climatic station, the calculations were performed for rangeland, wheat, and fallow conditions, each with their appropriate BMT and k-coefficients shown in Table 3-5, and for albedoes

TABLE 3-8

Energy Needed to Initiate Free Convection

May 24, 1974:

Station	ΔH (cal/cm^2)	
Omaha, Nebraska	66	
Topeka, Kansas	80	$\overline{\Delta H} = 79$
Dodge City, Kansas	90	

July 3, 1975:

Omaha, Nebraska	54	
Topeka, Kansas	14	$\overline{\Delta H} = 25$
Dodge City, Kansas	6	

July 5, 1975:

International Falls, Minnesota	35	
Bismarck, North Dakota	75	$\overline{\Delta H} = 55$

of fifteen, twenty, and twenty-five percent. Each station report was assigned to a polygon area of influence, drawn by the Thiessen polygon method. These polygons are shown drawn on Figures 2-6 to 2-8. The calculated soil moisture, evaporation, and available energy at the stations were then distributed in the polygon around each climatic station according to the rangeland and cultivated land distribution and to the average albedo of these surfaces. Figures 3-7 to 3-12 present the set of maps drawn for the 24 May case, Figures 3-13 to 3-18 show the maps for the 3 July case, and Figures 3-19 to 3-24 show the maps for the 5 July case. All maps are at 1:1,000,000 scale and therefore can be matched to the Landsat images in Figures 2-2, 2-4, and 2-5.

The solar and net radiation maps are for the morning hours of 24 May, 3 July, and 5 July, up to the times of the Landsat images. These are calculated by the methods illustrated in 3.2.1 assuming no cloud cover. The assumption is justifiable because the cloud cover is very little (except in the south portion of the 3 July image) and probably appeared only in the last hour prior to the image times. The net and solar radiations thus show a slight increase toward the east where the sun has been shining longer.

In the calculation of the total moisture left in the soil at the time of the Landsat images (Figures 3-9, 3-15, and 3-21), the net radiation R_{NET} is needed for estimating daily ETP and ET, and is therefore one of the driving parameters of the soil moisture budget subroutine. For these R_{NET} calculations we have used the cloud cover, wind, and dew point temperatures at Concordia for the two Kansas cases, and at Fargo for the Fargo case. These are the nearest stations having these parameters available on a six-hour basis.

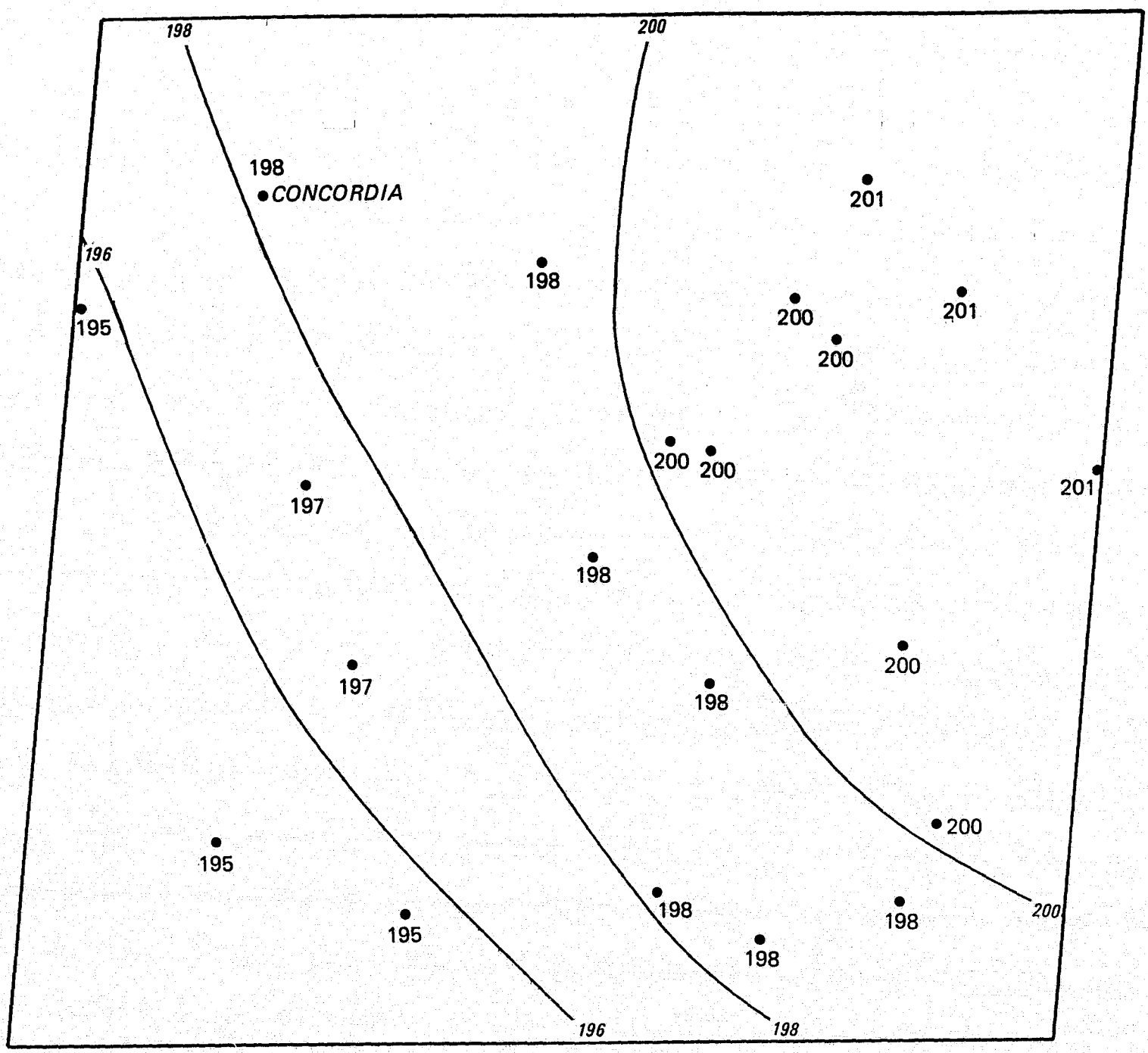

Figure 3-7: Solar radiation (cal/cm^2) received at each climatic station in the Manhattan, Kansas area the morning of 24 May 1974 from sunrise to the time of Landsat-1 passage.

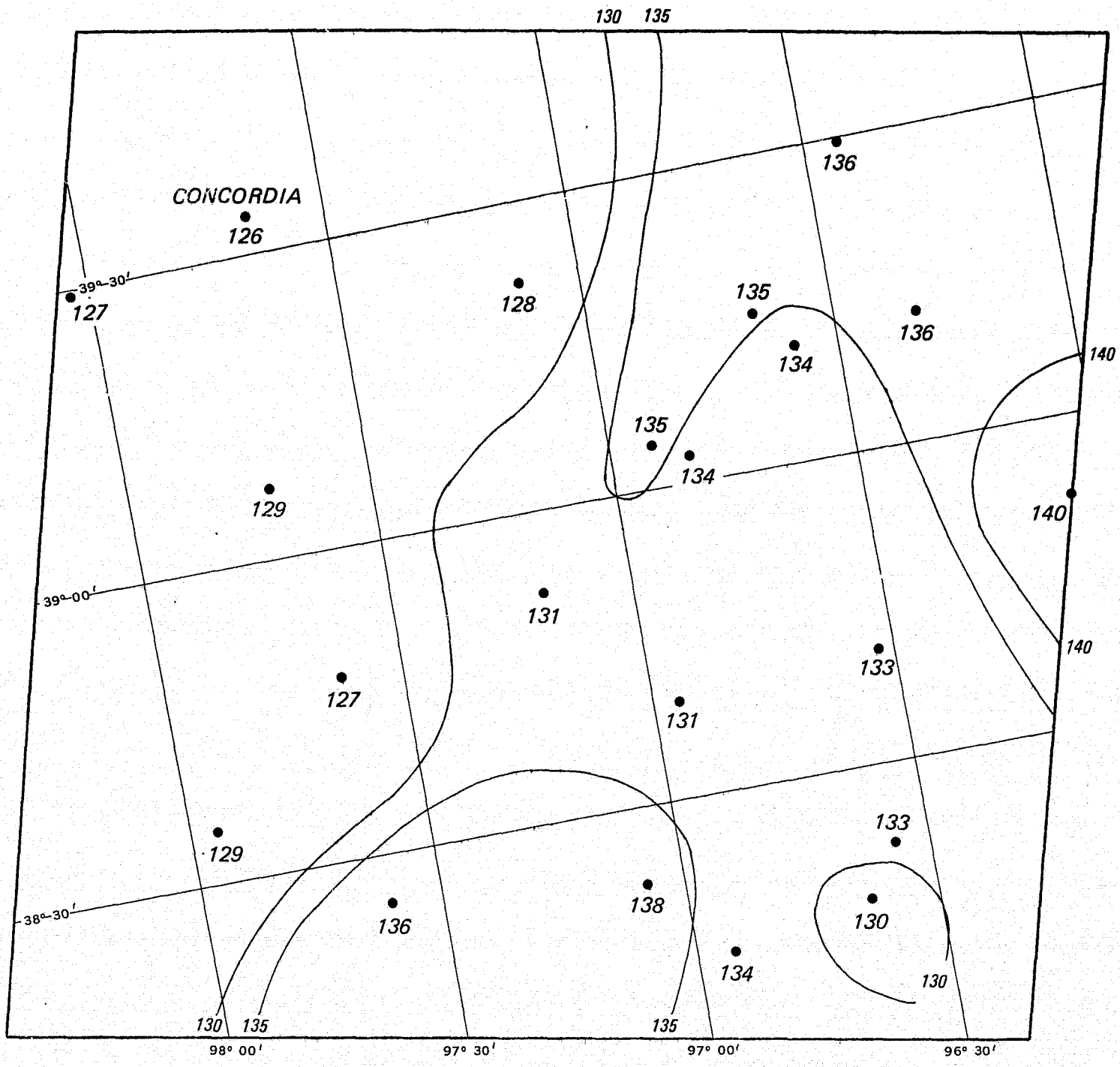

Figure 3-8: Net radiation (cal/cm^2) received at each climatic station in the Manhattan, Kansas area the morning of 24 May 1974 from sunrise to the time of Landsat-1 passage.

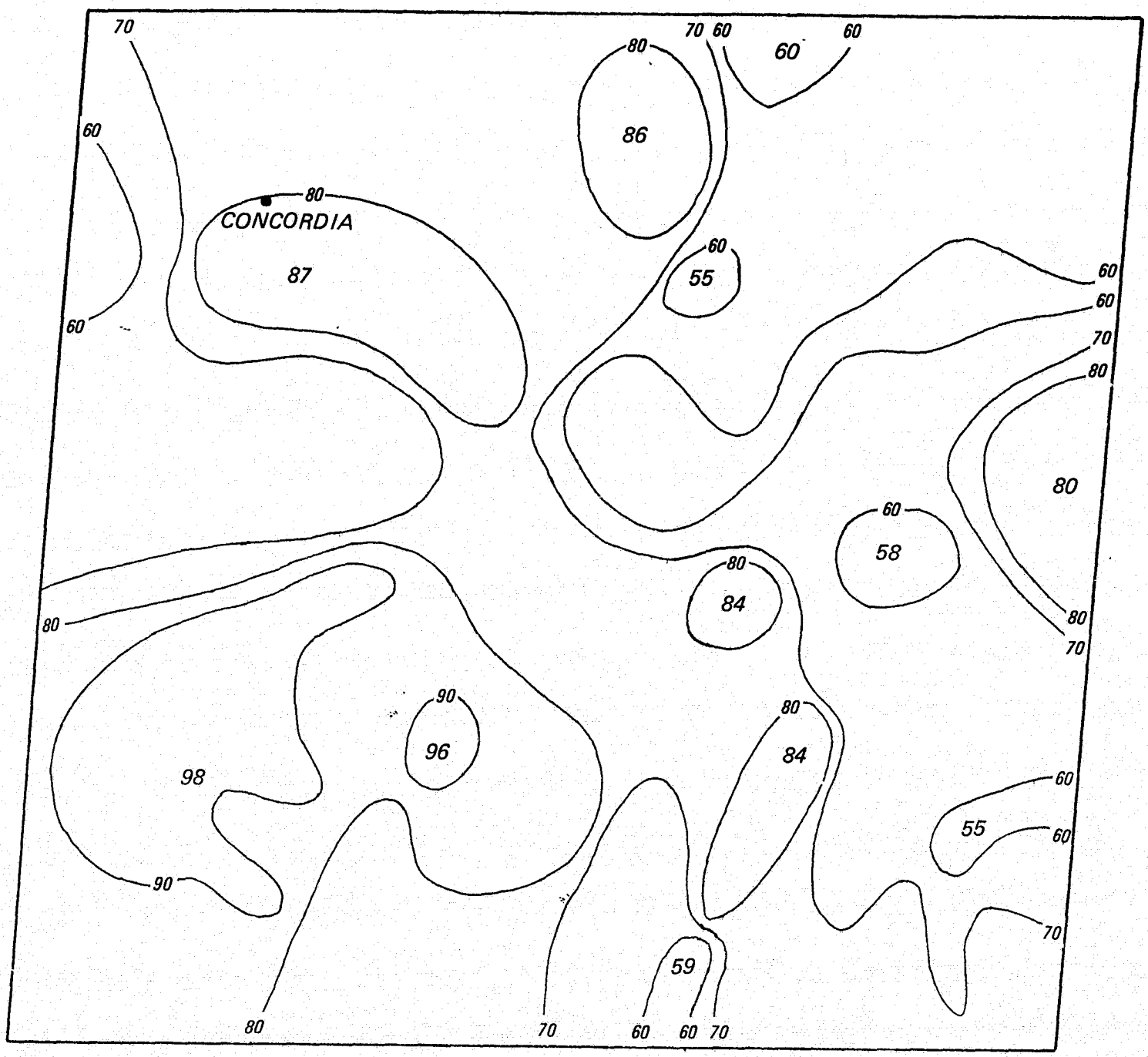

Figure 3-9: Total soil moisture (mm) in the Manhattan, Kansas area the morning of 24 May 1974.

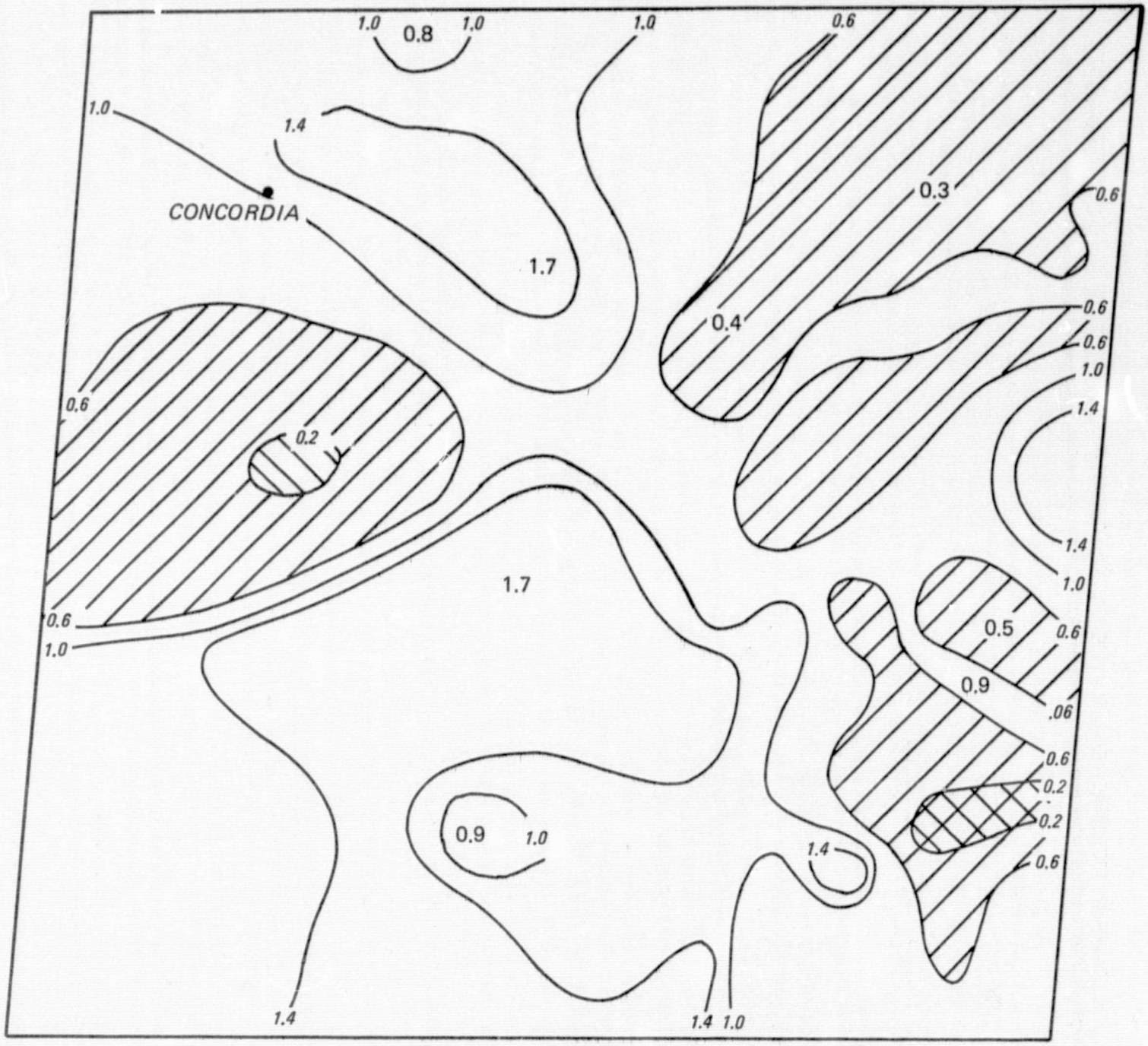

Figure 3-10: Total evaporation (mm) in the Manhattan, Kansas area the morning of 24 May 1974 from sunrise to the time of Landsat passage.

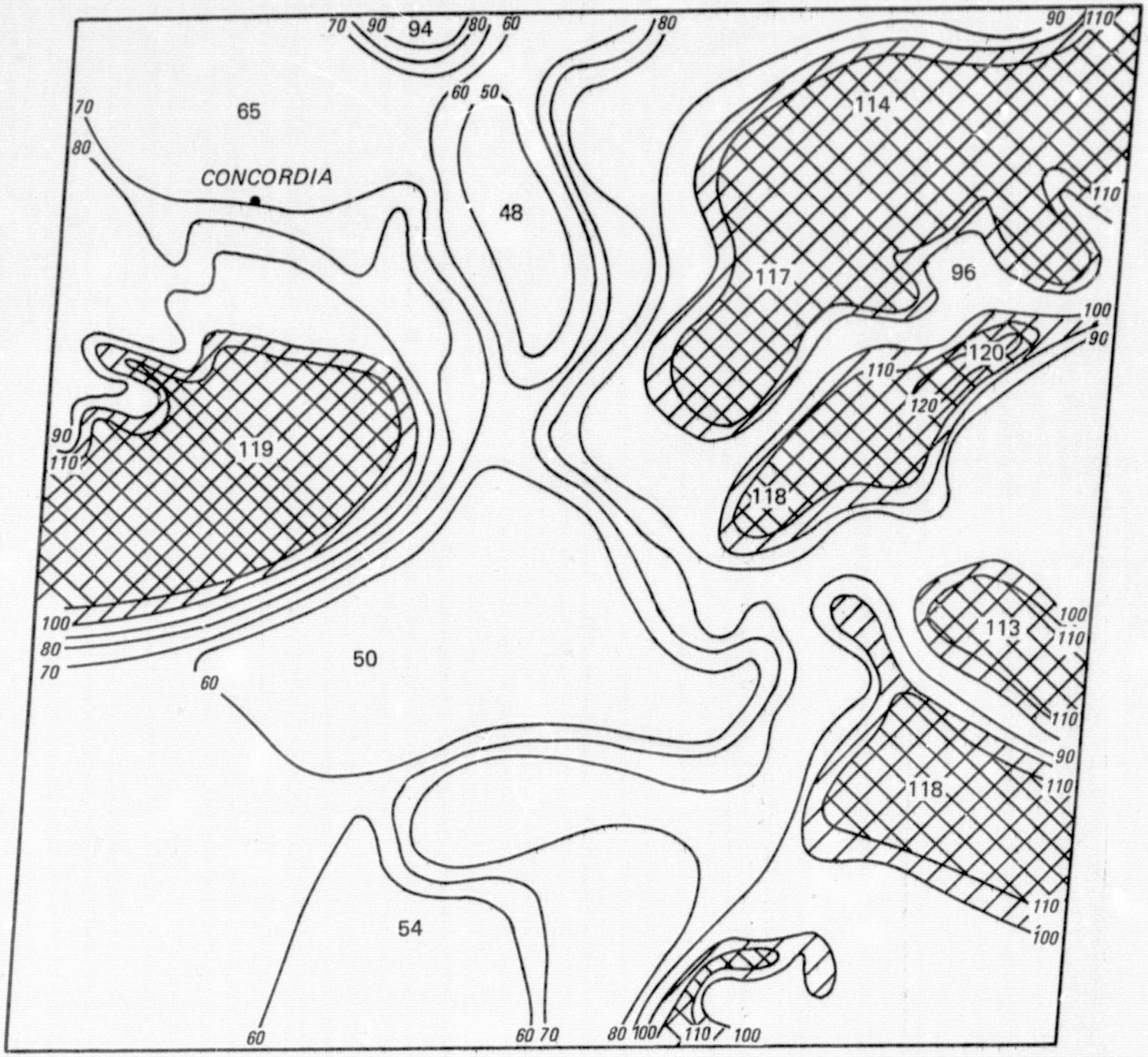

Figure 3-11: Total available energy to heat the air (cal/cm^2) in the Manhattan, Kansas area the morning of 24 May 1974 from sunrise to the time of Landsat passage.

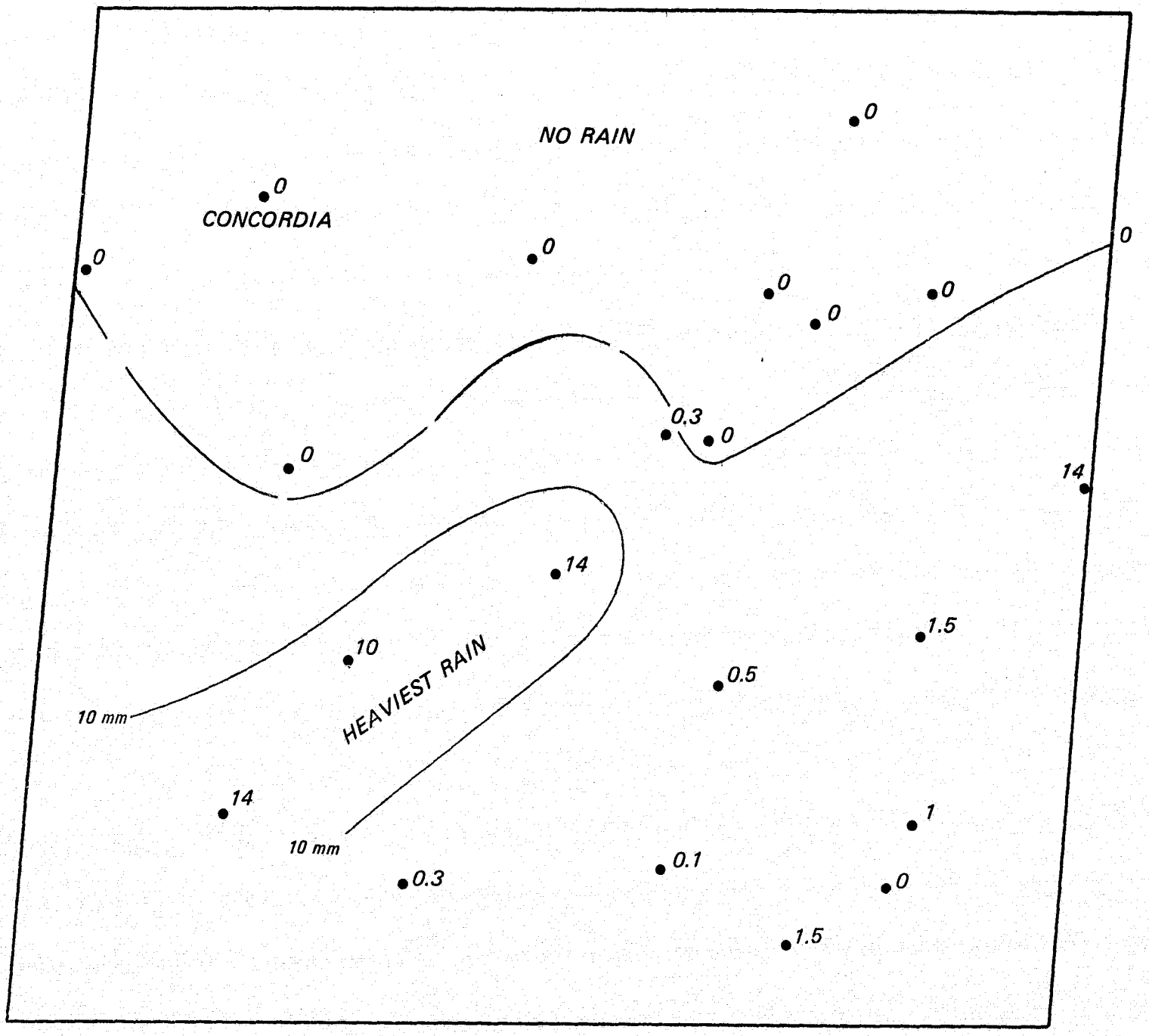

Figure 3-12: Total rain (mm) received in the Manhattan, Kansas area during 21-23 May 1974 (Kansas Climatological Data, NOAA National Climatic Center, May 1974).

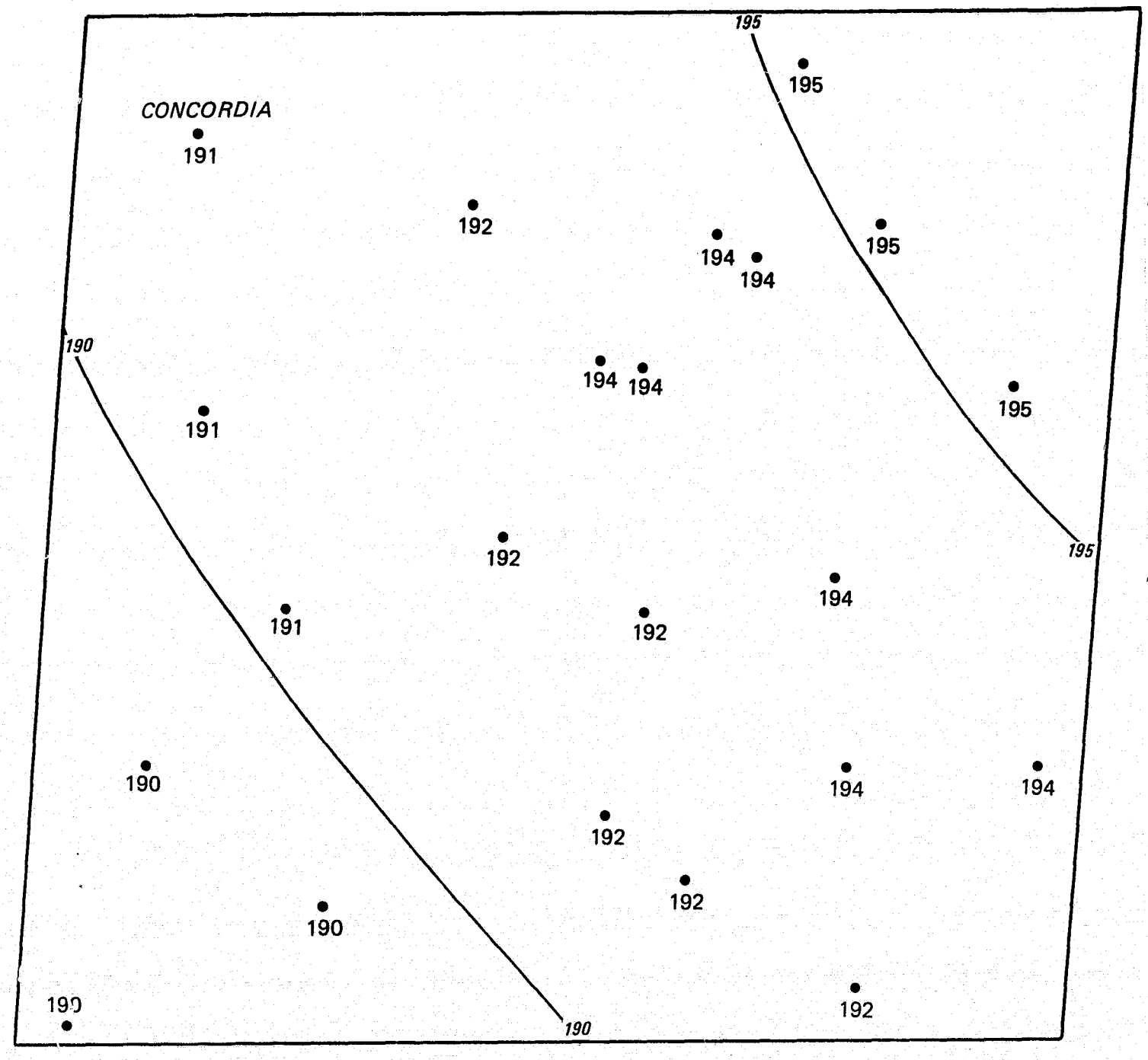

Figure 3-13: Solar radiation (cal/cm^2) received at each climatic station in the Manhattan, Kansas area the morning of 3 July 1975 from sunrise to the time of Landsat-1 passage.

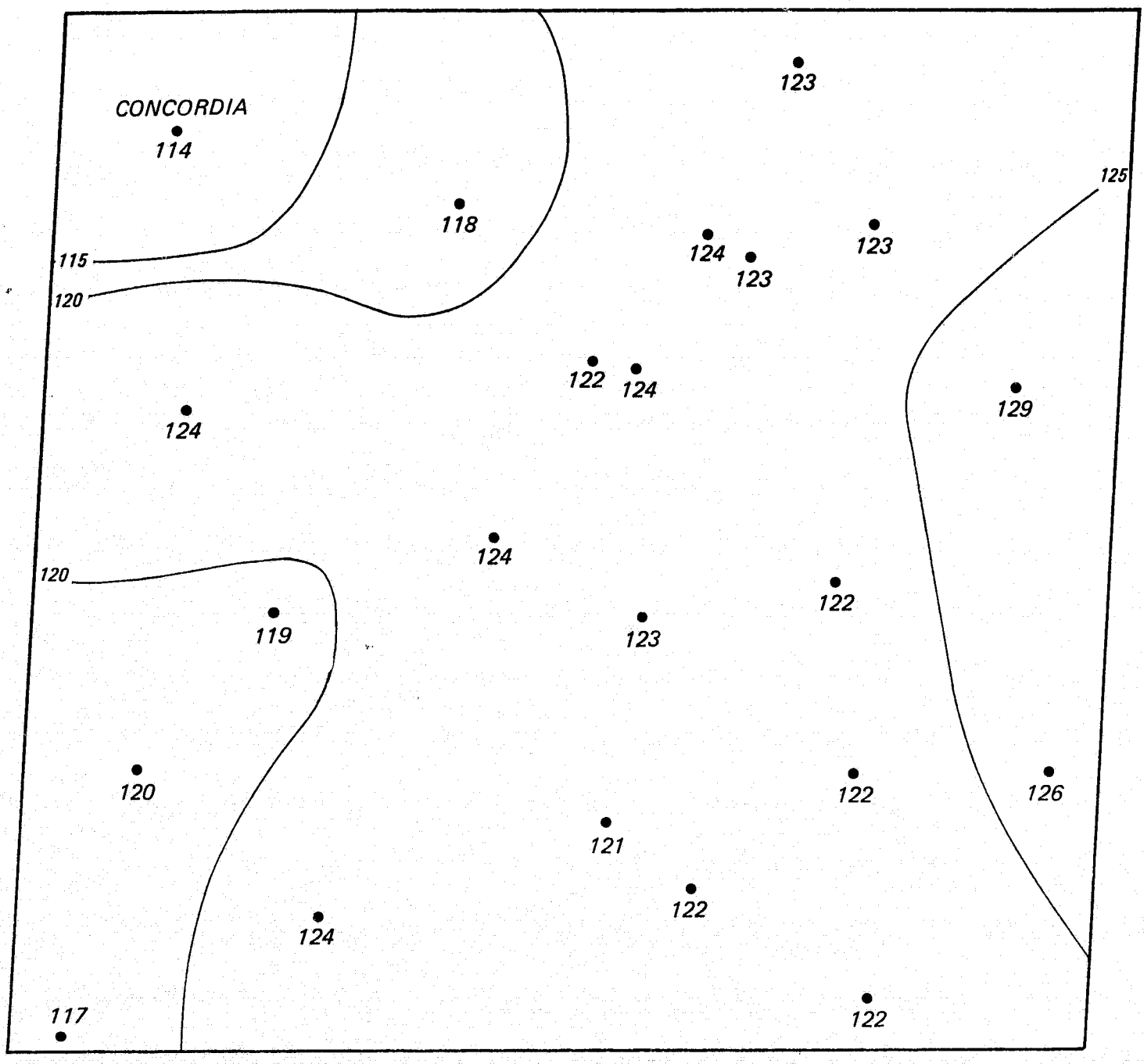

Figure 3-14: Net radiation (cal/cm^2) received at each climatic station in the Manhattan, Kansas area the morning of 3 July 1975 from sunrise to the time of Landsat-1 passage.

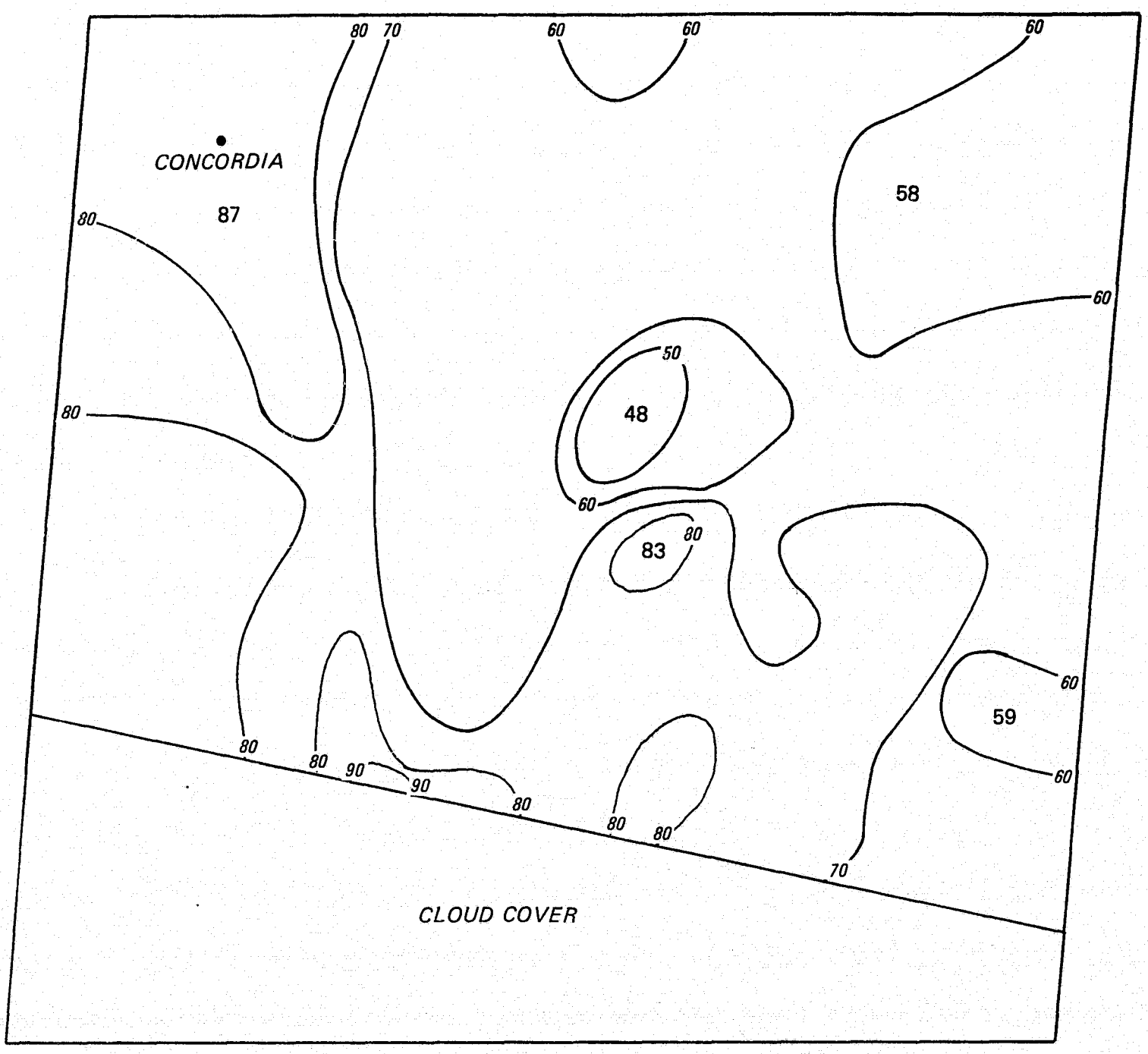

Figure 3-15: Total soil moisture (mm) in the Manhattan, Kansas area the morning of 3 July 1975.

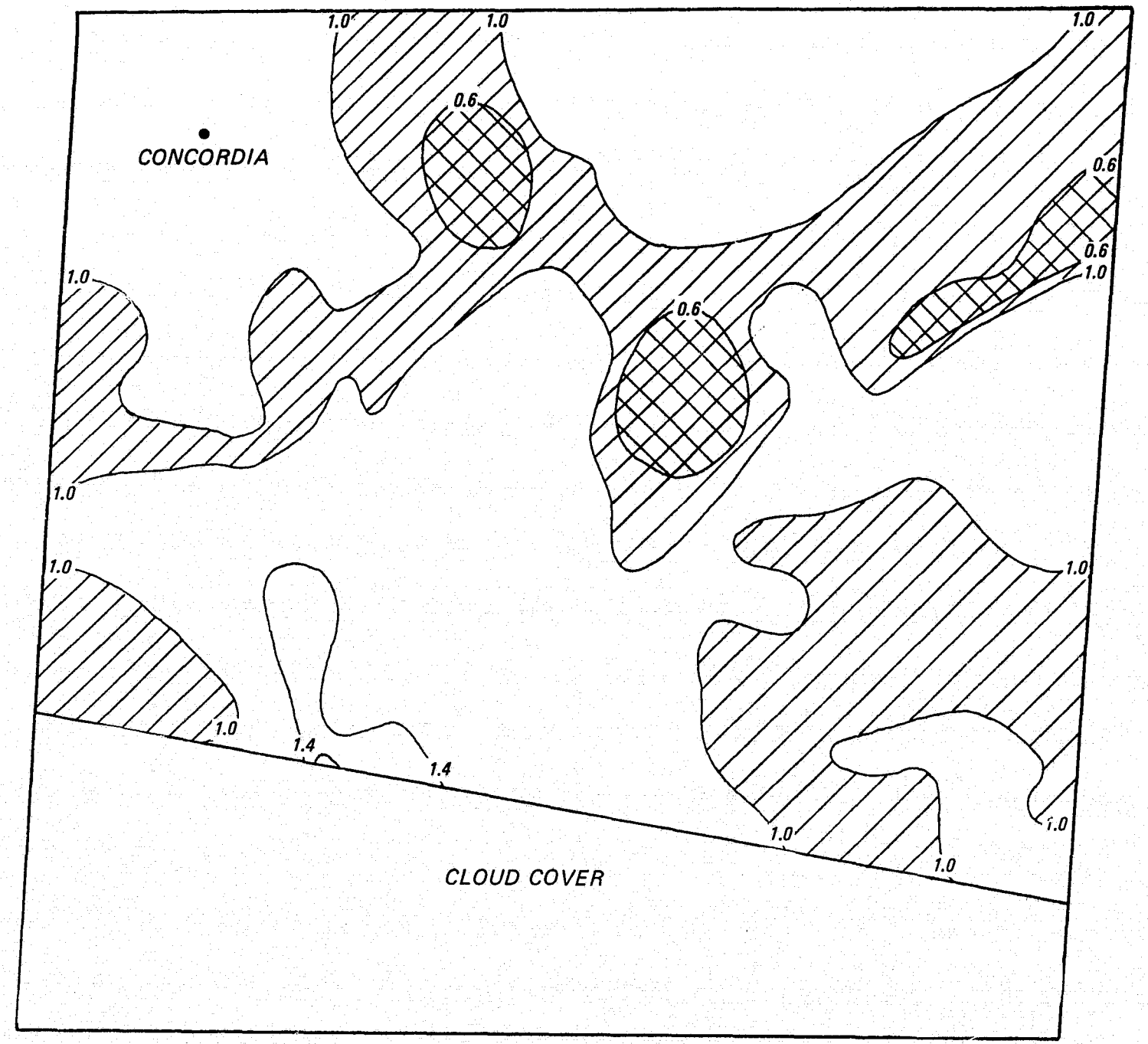

Figure 3-16: Total evaporation (mm) in the Manhattan, Kansas area the morning of 3 July 1975 from sunrise to the time of Landsat passage.

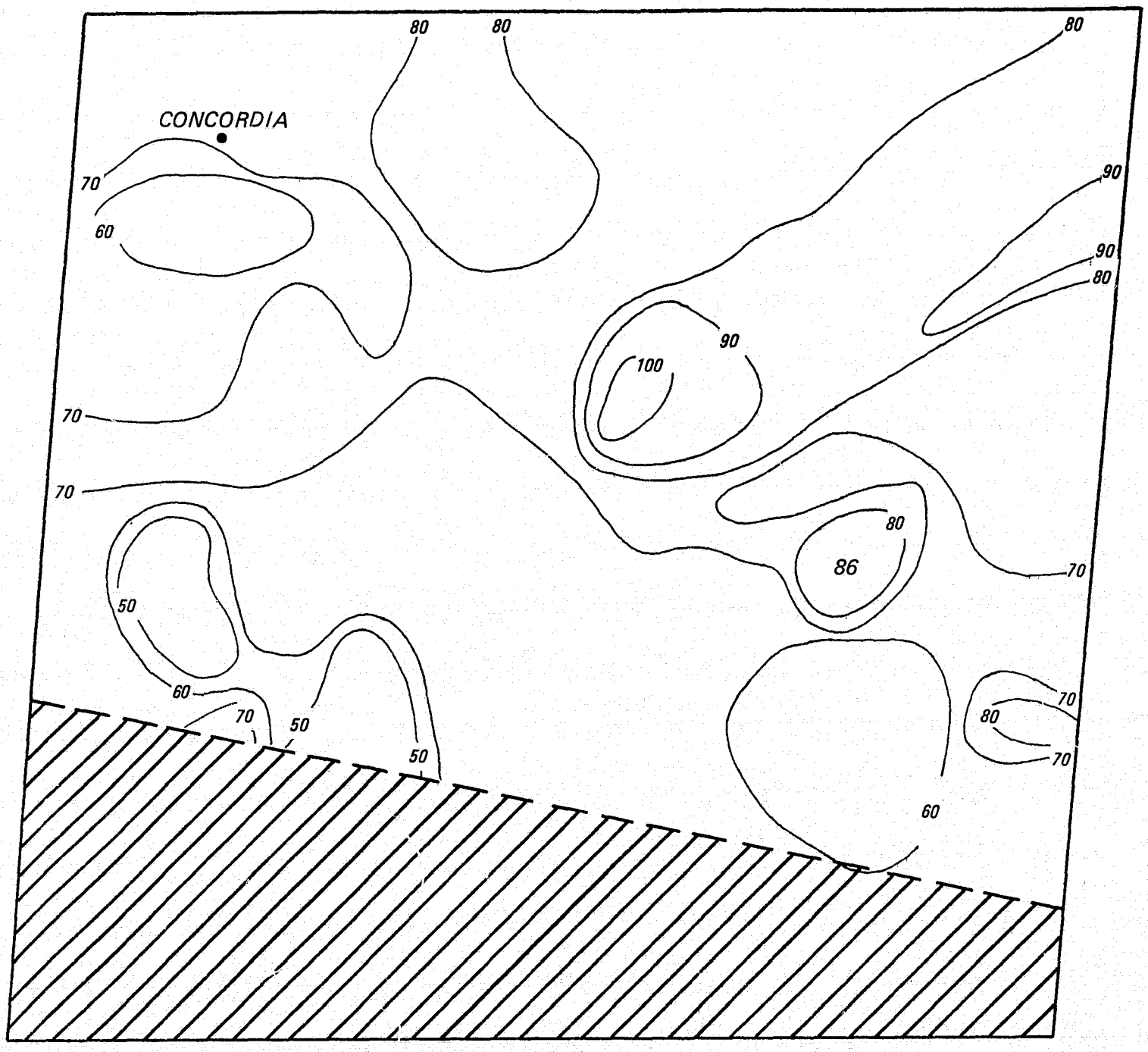

Figure 3-17: Total available energy to heat the air (cal/cm^2) in the Manhattan, Kansas area the morning of 3 July 1975 from sunrise to the time of Landsat image.

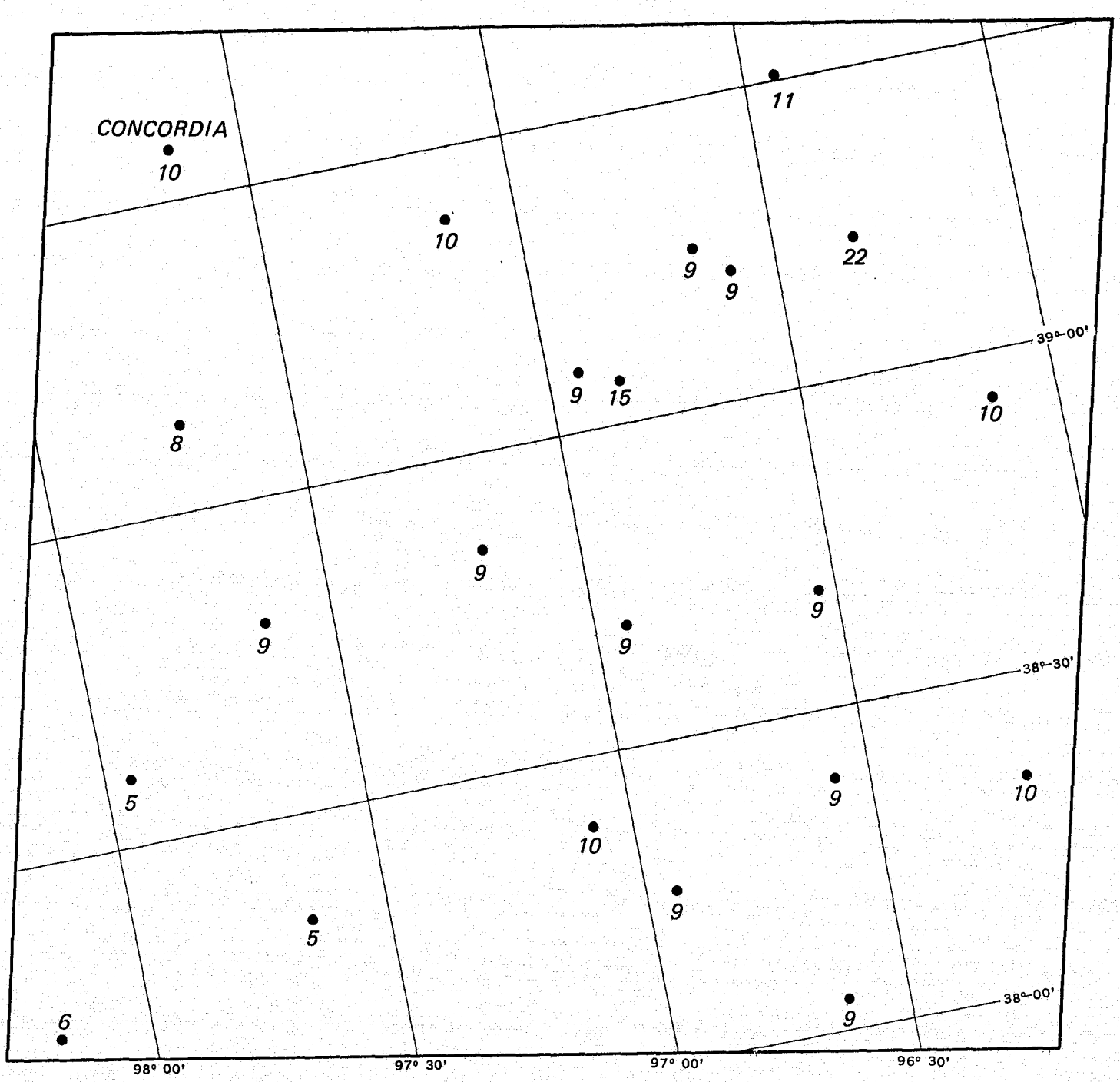

Figure 3-18: Days without rain prior to the morning of 3 July 1975 observed at climatic stations in the Manhattan, Kansas area (Kansas Climatological Data, NOAA National Climatic Center, June-July 1975).

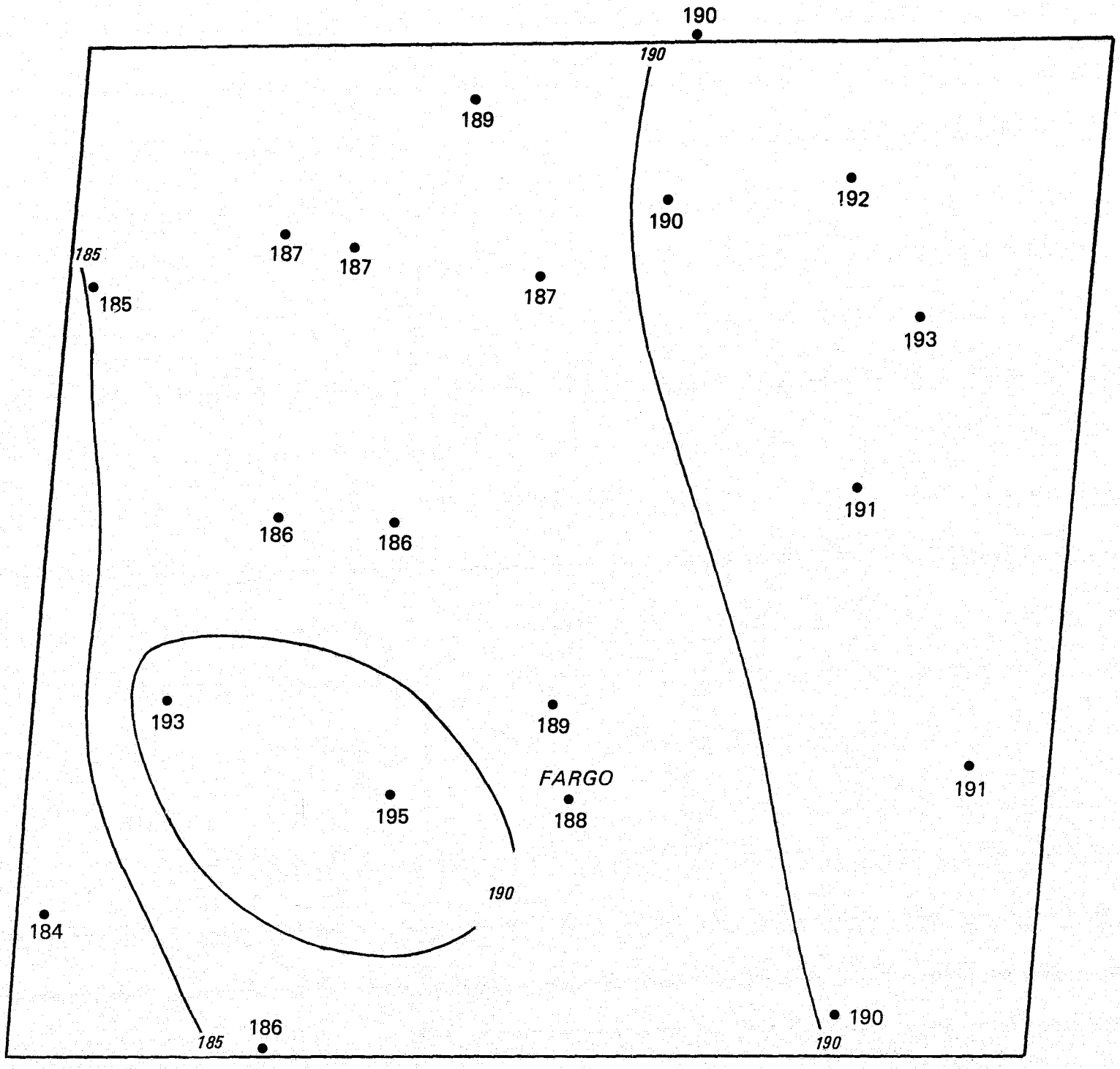

Figure 3-19: Solar radiation (cal/cm^2) received at each climatic station in the Fargo, North Dakota area the morning of 5 July 1975 from sunrise to the time of Landsat-1 passage.

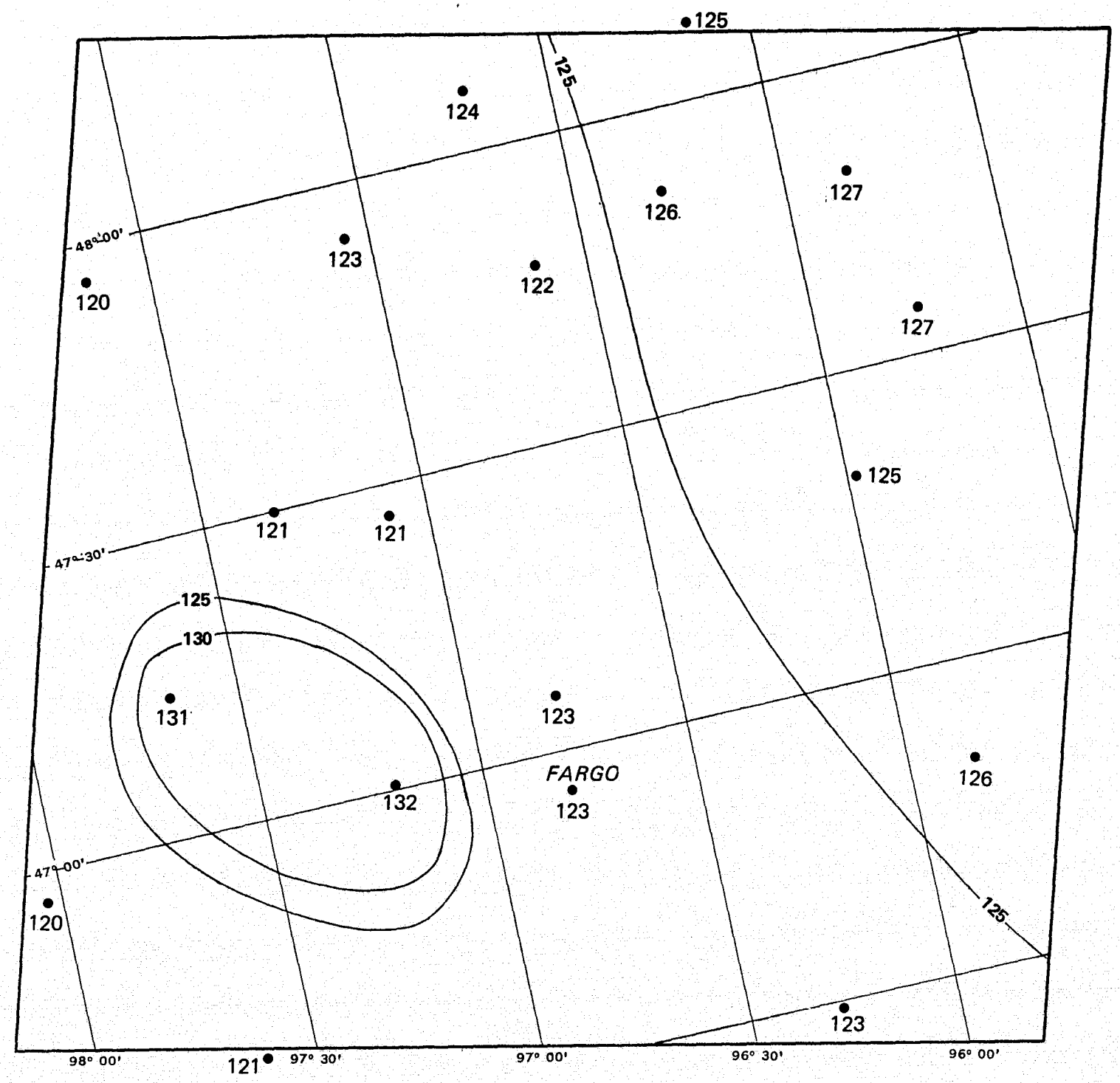

Figure 3-20: Net radiation (cal/cm^2) received at each climatic station in the Fargo, North Dakota area the morning of 5 July 1975 from sunrise to the time of Landsat-1 passage. An albedo of 20% was assumed in the calculations.

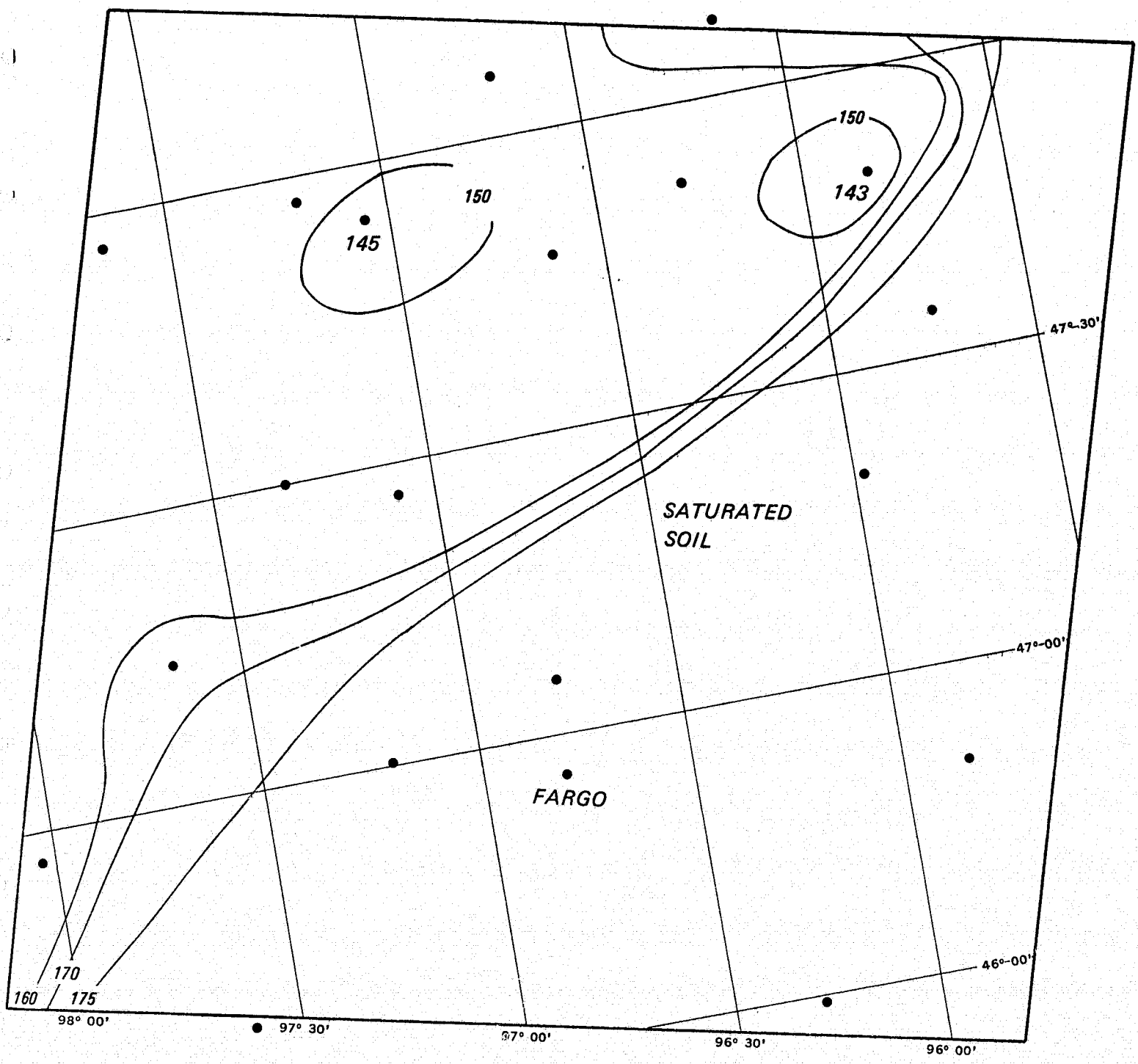

Figure 3-21: Total soil moisture (mm) in the Fargo, North Dakota area the morning of 5 July 1975. Values of 175mm reflect saturated and flooded conditions.

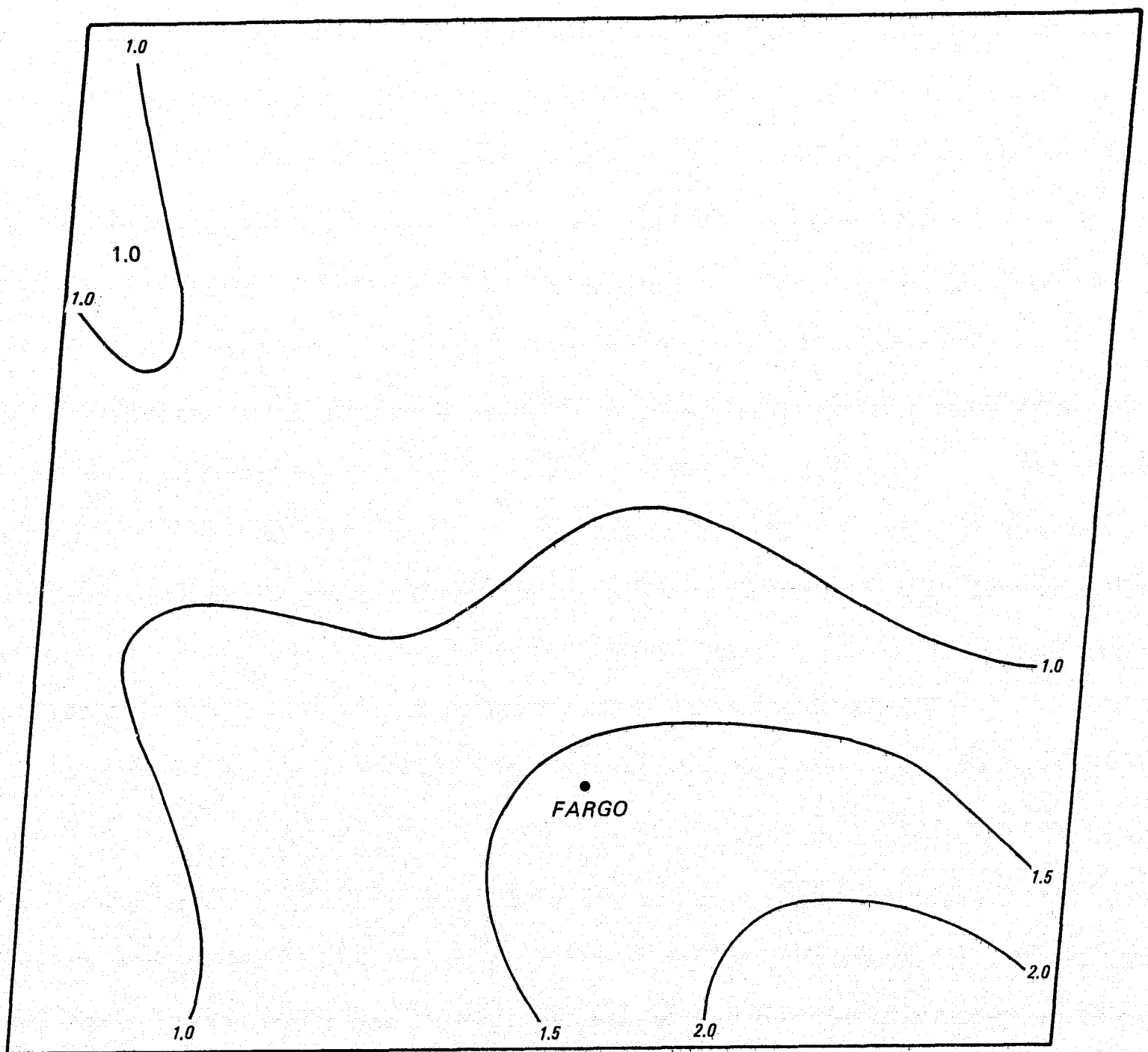

Figure 3-22: Total evaporation (mm) in the Fargo, North Dakota area the morning of 5 July 1975 from sunrise to the time of Landsat passage.

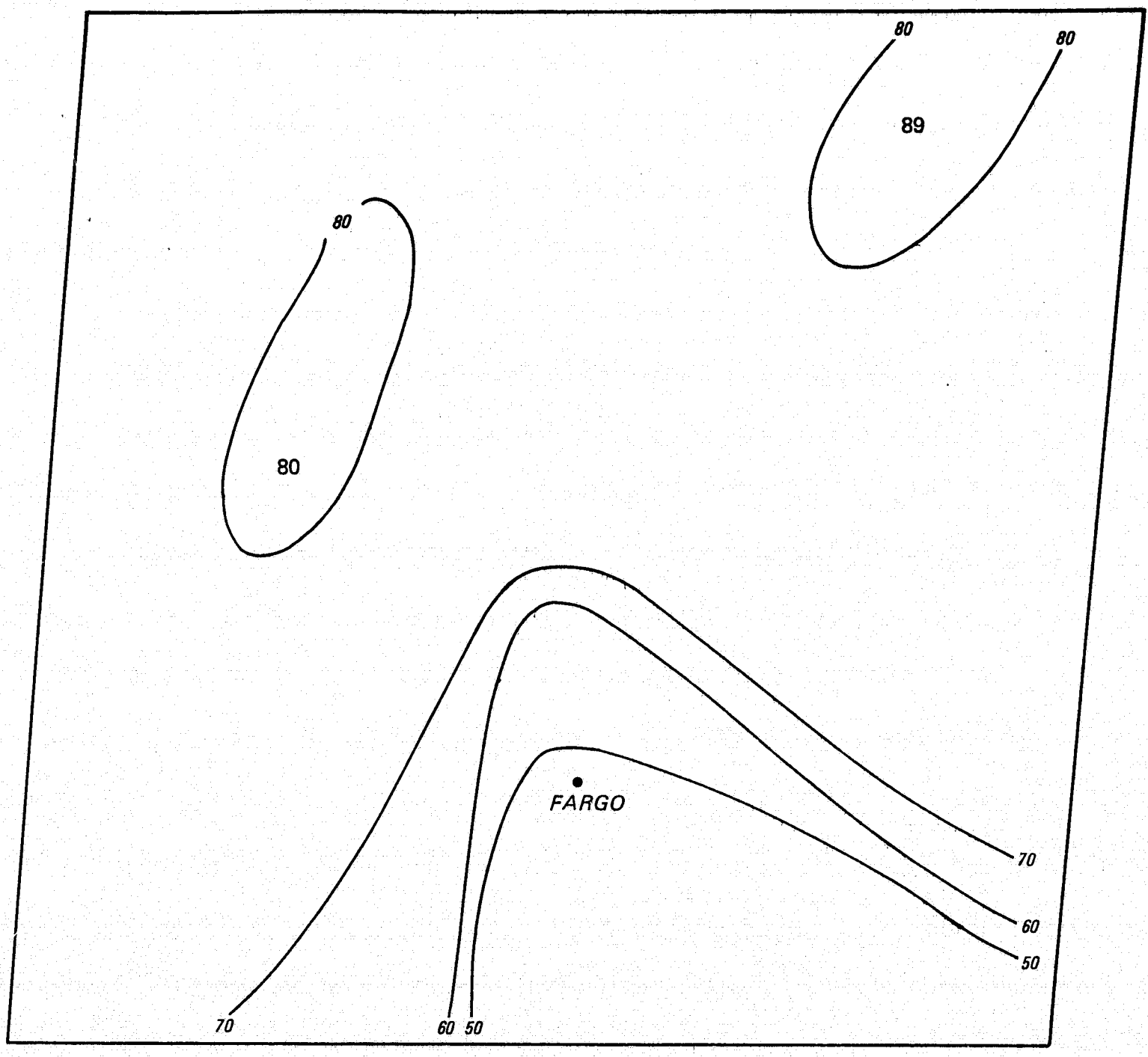

Figure 3-23: Total available energy to heat the air (cal/cm^2) in the Fargo, North Dakota area the morning of 5 July 1975 from sunrise to the time of Landsat passage.

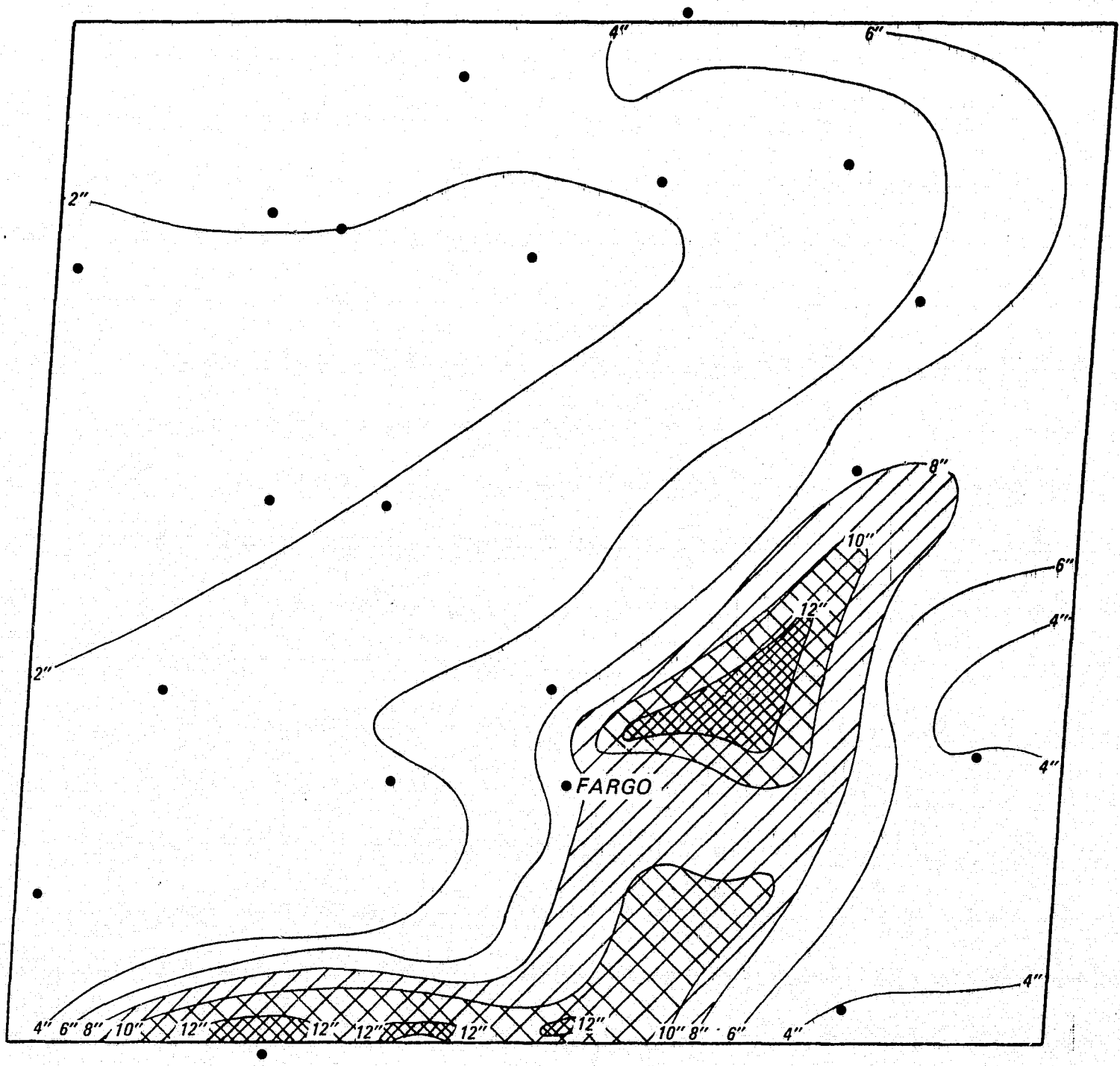

Figure 3-24: Total rain (inches) received in the period June 26 - July 5 1975 (North Dakota Climatological Data, NOAA National Climatic Center, August 1975).

The total soil moisture distribution reflects mostly the precipitation distribution of the previous days (shown in Figures 3-12, 3-18, 3-24), but is also influenced by the range and cultivated land distributions. Generally, the range seems to retain slightly more moisture than the wheat-cultivated fields.

The total ET (sunrise to time of Landsat image) is not only dependent on the available soil moisture, but also on the albedo, the type of surface cover, and the root structure (BMT and K-coefficients). The various combinations of these parameters produce the ET maps shown in Figures 3-10, 3-16, and 3-22.

Finally, the distributions of the energy available to heat air (Figures 3-11, 3-17, and 3-23) follow closely the ET distributions, with the highest energy available where the ET's are lowest.

The effects of surface cover are best illustrated by Tables 3-9, 3-10, and 3-11 which summarize the heat and soil moisture budget calculations averaged for all the climatic stations involved in the three cases of interest, for the different combinations of albedoes and ground conditions.

Fallow or recently harvested land which has no moisture demand from crops, retains moisture better than cultivated or grassland. It has the lowest evaporation, and therefore has the highest energy available to heat the air. For the three cases we considered, fallow conditions cause approximately seven percent and twenty percent more energy to be available to heat the air than rangeland and wheat fields respectively, but only the Kansas 3 July scene has sufficient fallow land to appreciably affect the moisture and heat budgets. We have estimated from the Kansas Weekly Weather-Crop Report published for the week of 7 July (U.S.D.A., 1975) that

TABLE 3-9

Summary of Results of the Heat and Soil Moisture Budget Calculations Averaged for All Climatic Stations (21), 24 May 1974 Case

	ALBEDO		
	15%	20%	25%
Solar Radiation (cal/cm^2)	198	198	198
Net Radiation (cal/cm^2)	143	133	123
Total Soil Moisture - Range	76	77	76
(mm) Wheat	63	64	65
Fallow	79	80	81
Total ET - Range	0.8	0.8	0.8
(mm) Wheat	1.2	1.1	1.1
Fallow	0.7	0.7	0.7
Energy for heating air (cal/cm^2) - Range	103	95	88
Wheat	85	80	70
Fallow	109	99	91

TABLE 3-10

Summary of Results of the Heat and Soil Moisture Budget Calculations Averaged for All Climatic Stations (22), 3 July 1975 Case

	ALBEDO		
	15%	20%	25%
Solar Radiation (cal/cm^2)	193	193	193
Net Radiation (cal/cm^2)	136	127	117
Total Soil Moisture - Range (mm)	71	73	75
Wheat	56	58	60
Fallow	91	93	94
Total ET - Range (mm)	1.0	1.1	1.2
Wheat	1.1	1.2	1.2
Fallow	1.0	.9	.8
Energy for heating air (cal/cm^2) - Range	85	73	57
Wheat	80	66	58
Fallow	87	81	74

TABLE 3-11

Summary of Results of the Heat and Soil Moisture Budget Calculations Averaged for All Climatic Stations (20), 5 July 1975 Case

		ALBEDO		
		15%	20%	25%
Solar Radiation (cal/cm^2)		189	189	189
Net Radiation (cal/cm^2)		134	124	115
Total Soil Moisture (mm)	Wheat	163	163	164
	Fallow	166	167	168
Total ET (mm)	Wheat	1.1	1.0	0.9
	Fallow	.9	.9	.8
Energy for heating air (cal/cm^2)				
	Wheat	73	71	67
	Fallow	86	80	73

approximately fifty percent of the wheat fields in the Landsat area of 3 July have recently been harvested and lay fallow. Since the wheat acreage is about seventy percent of total agricultural areas (Kansas State Board of Agriculture, 1976), about one-third of the total agricultural area is fallow on 3 July.

In general, higher albedoes (and therefore lower net radiation) cause the soil to retain slightly more moisture, and do not affect ET greatly if sufficient moisture is available in the soil, but the resulting lower net radiation causes correspondingly lower energies to be available to heat the air. For the three cases we analyzed, on the average a decrease of five percent in albedo causes an increase of about nine calories per cm^2 of energy available to heat the air.

Table 3-12 summarizes the budget calculation results averaged for the clear and cloudy areas. The averages shown in Table 3-12 were obtained by super-imposing a cloud cover map derived from the Landsat images on each of the soil moisture, evaporation, and available energy maps. Each parameter was spatially averaged for clear and cloudy areas. The results of this analysis do not show any distinct differences between cloudy and clear areas, although the cloudy areas do have slightly more available energy than the clear areas. A comparison of average energy available to heat the air (Table 3-12) to energy needed to overcome the morning inversion (Table 3-8), shows that in the 24 May and 5 July cases these are a few percentages of each other, while in the 3 July case the average energy contributed by the ground (73 cal/cm^2) greatly exceeds the average energy needed to overcome the inversion (25 cal/cm^2).

TABLE 3-12

Summary of Results of the Heat and Soil Moisture Budget Calculations Averaged for the Total Image Area and for the Clear and Cloudy Areas

	Total Area Average	Cloudy Area Average	Clear Area Average
May 24			
Soil Moisture (mm)	73	77	70
Evaporation (mm)	.93	.94	.92
Average Energy (cal/cm^2)	84	87	82
July 3			
Soil Moisture	69	70	66
Evaporation	1.02	1.10	.95
Average Energy	72	72	72
July 5			
Soil Moisture	167	165	167
Evaporation	1.04	.95	1.06
Average Energy	70	73	69

In the 3 July case convection, which tends to resolve itself into patterns of ascending and descending motions, is the predominant process producing the rows of thicker and more extensive clouds. Although, according to our budget calculations, sufficient heat is available over the entire Landsat image to overcome the morning inversion there are areas north of the Kansas River (upper center) and right of image where little or no clouds have formed. These areas seem to have lower reflectances in the MSS 5 channel than the cloudy areas and correspond more nearly to rangeland. Clouds have thus formed preferentially over cultivated lands, which because of their high percentage fallow conditions at this time of year, have a greater share of their heat budget to contribute to heat the air. Nevertheless, our heat budget calculations failed to show marked differences between cloudy and clear areas.

In the 24 May and 3 July cases, frictional mixing of the lower atmosphere due to surface roughness may be the prevalent process causing the random distribution of small cloud parcels. Additionally, flooded areas in the 3 July case increase the importance of the ground storage heat budget term neglected in our calculations.

Table 3-13 presents the results of an analysis of surface albedoes performed on the background image (6 May) of the 24 May case. Two cloudy areas and two clear areas as shown on the 24 May image were selected and average albedoes and standard deviations were computed from the 6 May image. The slightly higher standard deviations of the two clear areas indicate greater variations of surface cover which may be associated with greater surface roughness and possibly a greater percentage of fallow fields. These

TABLE 3-13

Average Albedoes and Standard Deviations of Selected Areas on the 6 May Background Image

Area*	Average Albedo	Stand. Dev.	No. of Samples	Conditions on 24 May Image
1	18.47	1.58	286	Cloudy
2	18.79	1.07	515	Clear
3	20.49	1.34	454	Cloudy
4	20.05	1.07	345	Clear

* The selected areas are indicated on Figure 2-1

conditions may be responsible for the appearance of small cumulus clouds in the 24 May case.

In the 5 July case, the inundated fields northeast of Fargo act in two ways to suppress cumulus formation: first, they provide a smooth surface which inhibits turbulent mixing; and second they become reservoirs to the radiant heat (just like a lake) making less heat available to heat the air. Our heat budget scheme does not provide for a heat storage term (which in the case of dry land is an order of magnitude less than the other budget term), and therefore fails to show the inhibiting effect of the flooded areas on the heat available for convection. Average energy available to heat the air as calculated by the budget (70 cal/cm^2) is a little less than that needed for free convection (75 cal/cm^2 at Bismarck). But in this case, where the surface heat storage is important, there would be even less energy available to heat the air. Thus, turbulent mixing becomes the important convective process and clouds would preferentially form in areas where turbulent mixing is most pronounced.

4.0 SUMMARY AND CONCLUSIONS

We have calculated the surface heat and moisture budget for three Landsat image areas in order to explore the relationship between air mass cumulus clouds and budget terms. To perform the calculations we employed modified computer subroutines from the EarthSat Cropcast System, meteorological data from climatological stations, and albedoes estimated from the Landsat data. The subroutines calculated net radiation, potential evapotranspiration (ETP) by the Penman method, and evapotranspiration (ET) by the Versatile Soil Moisture Budget (VB) method. The energy available to heat the air (L) in the morning of the Landsat image was estimated from the simple assumption that the net radiation energy left after what is used for evaporation would be employed to heat the ground surface which would ultimately transfer this heat to the air and possibly cause convective clouds to form. No provision was made for ground heat storage which in normal conditions is an order of magnitude less than heat employed in evaporation. It was also assumed that horizontal heat convection was negligible.

Only three types of surfaces were considered in our soil moisture budget calculations: wheat fields, grassland, and fallow fields, all characterized by a deep loam soil. The wheat and grass surfaces were given estimated growth stages characterized by a Biometeorological Time (BMT) and K-rooting coefficients. These growth stages were estimated from a knowledge of crop conditions at the dates of the Landsat images and were held constant for the entire image area.

The results of the budget calculations show that surface cover has the greatest control on evaporation and therefore on the amount of

energy, L, available to heat the air. Generally, fallow fields have lesser evaporation than either rangeland or cultivated fields, and therefore can provide a greater share of their heat budget to warm the air above. Albedo controls the net radiation and therefore also controls L. For the three cases under consideration a 5% change in albedo caused a 9 cal/cm^2 change in L accumulated during the morning hours prior to the Landsat image.

Areal averages of the budget components for clear and cloudy areas did not show any marked differences of soil moisture, evaporation, and L. There was, though, a weak correspondence between higher L's and cloud covered areas.

In two of the three cases analyzed (24 May, 5 July) the estimated L's averaged over the image area are about the same as the energy required to break the morning inversion as estimated from temperature soundings. In these two cases the Landsat images show a quasi-random distribution of small clouds characteristic of frictional mixing. An analysis of the background albedoes for the 24 May image showed a higher albedo standard deviation in cloudy areas. It is surmised that the greater albedo variation is indicative of greater surface roughness and/or greater percentage of fallow fields either of which would favor turbulent mixing and the appearance of small cumulus clouds. In the 5 July case, where frictional mixing is also thought to be the main cause of clouds, inundated fields act to suppress turbulent flow and cloud cover by reducing surface friction. Additionally, waterlogged surfaces evaporate at their maximum potential, have a much higher ground heat storage term (neglected in our budget calculations), and therefore offer less energy to heat the air than a normal surface.

In the third case studied (3 July) the estimated L averaged over the image area is considerably higher than the energy required to break the morning inversion, and the clouds are larger with a symmetrical row distribution typical of convective conditions. No difference is noticed in the average L of cloudy and clear areas, although clouds seem to form preferentially over agricultural areas in which 50% of the wheat has been harvested.

We believe that the weak correspondence between cloud cover and the moisture and heat budget terms may be due to two main reasons: 1) insufficient data to adequately describe spatially all parameters needed for the budget calculations, and 2) the coarseness of the surface heat and moisture budgets which assume no advection, no surface heat storage, and only 3 types of surface cover (wheat, grass, fallow conditions). In particular the exclusion of advection and the resulting frictional mixing of the lower atmospheric layers makes the model inadequate to account for small scale cumulus clouds variations such as those observed in the 24 May and 5 July Landsat images. Nevertheless, when advection is negligible the model may suffice for estimating the heat and moisture contributed by the surface to the air over an area as large as the Great Plains, and therefore can follow the day-to-day air mass modifications.

Some refinements that are readily implementable are 1) an inclusion of a surface heat storage term; 2) utilization of surface albedo to define water bodies and inclusion of these in the areal budget calculations; 3) better definition of surface vegetation conditions possibly through Landsat images; 4) calibration of the soil moisture budget against lysimeter measurements; 5) calibration of the solar radiation estimation against pyranometer measurements. Additionally the data base for the

budget calculations may be greatly augmented by the use of, 1) satellite measured surface skin-temperatures which in conjunction with surface temperature observations would afford a much higher spatial resolution of surface temperature for evaporation and net radiation calculations; 2) satellite observed cloud cover distribution for a better estimate of net radiation and possibly precipitation.

Our surface heat and moisture budget models can serve as the basis for more complex models of surface-air heat and moisture exchanges which would utilize readily available meteorological data and which would be applicable on a meso-scale.

5.0 RECOMMENDATIONS

The resources available to this study permitted only a limited examination of air mass to surface exchange processes. Nevertheless, a surface heat and moisture budget model has been developed that can form the basis for more complex models to be used to evaluate and perhaps parameterize heat budget factors on a scale as large as the U.S. Great Plains. Specific recommendations for further study include:

1. Improvements in the surface heat and soil moisture budget models.
2. Improvements in the data base and model calibration.

The improvements in the heat and moisture budget models can be achieved by inclusion of a ground heat storage term, a horizontal heat transport, and a turbulent mixing term to include horizontal mass convection and surface roughness. The data base for any future work should include meteorological satellite data and more extensive ground observations of evaporation, and solar radiation. The visible and infrared observations from the meteorological satellites would assist in estimating solar radiation, and precipitation. The infrared measurements, properly corrected for the atmosphere and surface emissivity, could provide surface temperatures in clear areas, which can then be used to improve surface net radiation and evaporation estimates.

The limited study undertaken, herein, has opened the door on a number of potential uses for Landsat and other remote sensing system in agriculture and meteorology. Additional studies should be initiated in the future. Emphasis in the future should, however, be directed toward the meteorological satellite applications since Landsat observational period is too restrictive.

REFERENCES

Baier, W. and G.W. Robertson, 1966. A new versatile soil moisture budget. Canadian J. Plant Sci. 46:299-315.

Baier, W., Chaput D.Z., Russello, D.A., and W.R. Sharp, 1972. Soil Moisture Estimator Program System. Tech. Bull. 78, Agrometeorology Section, Plant Research Institute, Research Branch, Canada Dept. of Agriculture.

Earth Satellite Corporation, 1975. EarthSat Spring Wheat Yield System Test 1975. Mid-term Report under Contract NAS9-14655, prepared for L.B. Johnson Space Center, Houston, Texas.

Earth Satellite Corporation, 1976. EarthSat Spring Wheat Yield System Test 1975. Final Report under Contract NAS9-14655, prepared for L.B. Johnson Space Center, Houston, Texas.

Elterman, L., 1968. UV, Visible, and IR Attenuation for Altitudes to 50 km. Air Force Cambridge Research Laboratories, AFCRL-68-0153.

Freund, J.E., 1970. Statistics, A First Course. Prentice-Hall, Inc., Englewood Cliffs, New Jersey.

Geiger, R., 1971. The Climate Near the Ground. Harvard University Press, Cambridge, Massachusetts.

General Electric, 1972. NASA Earth Resources Satellite, Data Users Handbook, Appendix A (Revised May 4, 1972). Prepared under Contract NAS5-11320 for NASA, Goddard Space Flight Center, Greenbelt, Maryland.

Kansas State Board of Agriculture, 1976. Farm Facts 1975-1976.

Klein, W.H., 1948. Journal of Meteorology, vol. 5, p. 119.

List, R.J., 1966. Smithsonian Meteorological Tables, Sixth Revised Edition, Smithsonian Institution, Washington, D.C.

Moon, P., 1946. Proposed Standard Solar Radiation Curve for Engineering Use. J. of Franklin Inst., 30, 583-619.

Penman, H.L., 1948. Natural evaporation from open water, bare soil, and grass. Proceedings of the Royal Society of London. 193, 120-145.

Penman, H.L., 1956. Evaporation: An Introductory Survey. Neth. J. Agricultural Science, vol. 4., pp. 9-29.

Sabatini, R.R. and G. Rabchevsky, 1970. Use of Ground-Truth Measurements to Monitor ERTS Sensor Calibration, Allied Research Associates, Inc., prepared under Contract No. NAS5-10342. Technical Report No. 16, Vol. II, for NASA/GSFC, Greenbelt, Md.

Saucier, W.J., 1955. Principles of Meteorological Analysis. The University of Chicago Press, Chicago and London.

U.S. Department of Agriculture, 7 July, 1975. Kansas Weekly Weather-Crop Report.

Williams, D.L., and B.L. Barker, 1974. Kansas Land-use Patterns. Map at 1:1,000,000 scale. Prepared by Space Technology Laboratories, U. of Kansas, Lawrence, Kansas.